DEVELOPMENT OF A NEW PARKINSON'S DISEASE MODEL USING ZEBRAFISH TO STUDY ALPHA-SYNUCLEIN AGGREGATION

A THESIS SUBMITTED TO
THE GRADUATE SCHOOL OF ENGINEERING AND SCIENCE
OF BILKENT UNIVERSITY
IN PARTIAL FULFILLMENT OF THE REQUIREMENTS FOR
THE DEGREE OF
MASTER OF SCIENCE
IN
MATERIALS SCIENCE AND NANOTECHNOLOGY

By
Elif Akış
August 2024

DEVELOPMENT OF A NEW PARKINSON'S DISEASE MODEL USING ZEBRAFISH TO ALPHA-SYNUCLEIN AGGREGATION

By Elif Akış

August 2024

We certify that we have read this thesis and that in our opinion it is fully adequate, in scope and in quality, as a thesis for the degree of Master of Science.

Fatih İnci (Advisor)

Ayça Arslan Ergül (Co-Advisor)

Aykut Erbaş

Gamze Bora Akoğlu

Approved for the Graduate School of Engineering and Science:

Orhan Arıkan

Director of Graduate School

ABSTRACT

DEVELOPMENT OF A NEW PARKINSON'S DISEASE MODEL USING ZEBRAFISH TO STUDY ALPHA-SYNUCLEIN AGGREGATION

Elif Akış

M.S. in Material Science and Nanotechnology

Supervisor : Fatih İnci

Co-Advisor : Ayça Arslan Ergül

August 2024

Parkinson's Disease is a neurodegenerative disease mainly caused by the dopaminergic neuron loss in the CNS, specifically substantia nigra. It progresses through three stages: preclinical, prodromal, and clinical. Patients with Parkinson's disease experience motor symptoms like tremors, postural problems and rigidity as well as non-motor symptoms such as autonomic dysfunction, sleep disorders, and depression. Various genetic and environmental factors influence the disease's progression, making classifying patients based on disease pathology challenging. The SNCA gene encodes the alpha-synuclein protein and is a primary risk factor for Parkinson's disease. Mutant forms of alpha-synuclein can form insoluble fibrils and Lewy bodies, affecting the transmission of healthy proteins between cells. Recent hypotheses suggest that the location of disease emergence in the body (brain-first or body-first) influences disease progression and resulting pathology. Existing zebrafish models have the potential to provide insights into neurodegenerative diseases due to their ease of handling, large population size, and

genetic manipulability. This study aims to investigate the relationship between the location of alpha-synuclein emergence and the progression of Parkinson's disease. In this study, a new zebrafish model expressing the human alpha-synuclein coding sequence was developed using the Tol2 transposase-based recombination system. The initial expression vector was created using multisite gateway cloning methodology, and the constructs were validated at each step using PCR and sequencing. The final construct was co-injected with transposase mRNA into one-cell stage zebrafish embryos to facilitate the formation of a stable line. In addition, human alpha-synuclein fibril injections were performed on young and old zebrafish, either brain or gut. This way, we ensured the transmission of α-syn between the central nervous system and peripheral organs.

Keywords: *Parkinson's Disease, Zebrafish, Transgenesis, Neurodegenerative diseases, alpha-synuclein*

ÖZET

ZEBRA BALIĞI KULLANILARAK YENİ BİR PARKİNSON HASTALIĞI MODELİNİN GELİŞTİRİLMESİ VE ALFA SİNÜKLEİNİN ROLÜ

Elif Akış

Malzeme Bilimi ve Nanoteknoloji, Yüksek Lisans

Tez Danışmanı : Fatih İnci

İkinci Tez Danışmanı : Ayça Arslan Ergül

Ağustos 2024

Parkinson Hastalığı, özellikle substantia nigra (kara madde) olmak üzere merkezi sinir sistemindeki dopaminerjik nöronların kaybından kaynaklanan nörodejeneratif bir hastalıktır. Hastalık üç safhadan oluşur: klinik-öncesi, prodromal ve klinik. Parkinson hastalığı olan hastalarda titreme, sertlik ve postural dengesizlik gibi motor semptomların yanı sıra otonomik disfonksiyon, uyku bozuklukları ve depresyon gibi motor olmayan semptomlar da görülür. Hastalığın ilerlemesi çeşitli genetik ve çevresel pek çok faktörden etkilenerek hastalarda hastalık patolojisini ve evresinin sınıflandırılmasını zorlaştırmaktadır. Alfa-sinüklein proteinini kodlayan SNCA geni, Parkinson hastalığı için birincil risk faktörü olarak kabul edilmektedir. Alfa-sinükleinin mutant formları, çözünmeyen fibrillerin ve Lewy cisimciklerinin oluşumuna yol açarak nörodejenerasyona ve fibrillerin sağlıklı hücrelere yayılımına neden olmaktadır. Son

çalışmalar, hastalığın vücutta ortaya çıktığı yerin (önce beyin veya önce vücut), hastalığın ilerlemesini ve sonuçta ortaya çıkan patolojiyi etkilediğini ileri sürmektedir. Zebrabalığı hastalık modelleri, kullanım kolaylığı, popülasyon büyüklüğü ve genetik manipüle edilebilirliğin kolay olması nedeniyle nörodejeneratif hastalıklara ilişkin içgörü sağlama potansiyeline sahiptir. Bu çalışma, alfa-sinüklein patolojisinin vücutta başlama yeri ile Parkinson hastalığının ilerlemesi arasındaki ilişkiyi anlamayı amaçlamaktadır. Bu amaç doğrultusunda, Tol2 transpozaz bazlı rekombinasyon sistemi kullanılarak insan alfa-sinüklein kodlama dizisini ifade eden yeni bir zebra balığı modeli geliştirilmiştir. Çok bölgeli klonlama metodolojisi kullanılarak insan alfa-sinükleini içeren ekspresyon vektörü oluşturulmuştur. Bu vektör polimeraz zincir reaksiyonu (PZR) ve sekanslama kullanılarak her adımda doğrulanmıştır. Nihai plazmid, stabil bir ekspresyon oluşumunu kolaylaştırmak için tek hücreli aşama zebra balığı embriyolarına transpozaz mRNA ile birlikte enjekte edilerek stabil transgenik hat oluşumu sağlanmıştır. Ayrıca genç ve yaşlı zebrabalıklarına beyin veya bağırsaktan insan alfa-sinüklein fibril enjeksiyonları yapılarak, beyin ve vücut arasındaki alfa-sinüklein iletiminin olup olmadığı zebrabalığı beyin ve bağırsak dokularında incelenmiştir.

Anahtar kelimeler: *Parkinson Hastalığı, Zebrabalığı, Transgenik modelleme, Nörodejeneratif hastalıklar, alfa sinüklein*

To my family…

Acknowledgements

Firstly, I would like to express my deepest gratitude to my co-advisor Dr. Ayça Arslan Ergül. She is the most understanding, caring, and brilliant PI every student could dream of. I was so lucky to have a chance to work under her supervision on such advanced projects. Due to her trust in my potential, I was able to express my ideas freely and improve myself as a life scientist. I enjoyed working with her during these three years, and I became an independent, self-confident person. I want to express my sincere thanks to Dr. Fatih İnci as my supervisor. I deeply admire the efforts that he performed and spent his time to be a part of my master's journey. Also, I would like to thank my valuable jury members, Dr. Gamze Bora Akoğlu and Dr. Aykut Erbaş, for their time and consideration and for accepting to participate in my thesis defense jury.

During my master's, one of the biggest supporters were my labmates Tuba Sena Oğurlu and Elif Sena Temirci. I was so lucky to share this incredible journey with them; they became my little sisters and brilliant co-workers. In such a supportive team, we grew so much and developed our skills not only in science but also in personality. I would especially like to thank Ayşe Reyyan Kutan and Eylül Gülşen Yılmaz for their support, friendship, and great help through the process. They brought new perspectives and joy to my life, and I am grateful to have gained such valuable people. I would also like to thank all members of Arslan-Ergül Lab, namely Ceylin Çetinkaya, Bora Deniz Yılmaz, Umutcan Kaan Bozan, Ceren Aydoğan, Ali Eren Yüksel for their support. I became a big sister of the lab in such a young, smart, and dynamic team, yet I learned so much from

them. I want to credit İnci Lab and Adams Lab members for their great help during my studies. Before starting my master's, I met two excellent scientists, Gizem Geçgil and Esma Demirel. We began as colleagues and eventually became best friends, and they have played an immense role in my life. They have always supported me in every possible way with their presence and joy. I wanted to thank these two amazing people for their lifetime support and love.

I want to express my most incredible gratitude to my biggest supporter throughout my career, my dear love, Emin Berksun Ceryan. Thanks to him, I always found the courage to pursue my dreams. He always pulled me up in my bad times and cheered me for my success. I am so lucky to have him as a partner and soulmate in my life. Last but not least, I would like to thank my lovely family for their unwavering support and belief in any way. Thanks to them, I had the chance to pursue my dreams, and their love has been a constant source of strength and inspiration in my life.

Lastly, I would like to thank the TÜBİTAK (Scientific and Technological Research Council of Türkiye) for their invaluable support of our study. Funding is provided through the TÜBİTAK 2021-JPND-Widening grant named PD-PAM. (no: 122N005), enabled us to carry out the experiments that formed the basis of this thesis.

Content

LIST OF FIGURES ..... **XII**

LIST OF TABLES ..... **XIV**

CHAPTER 1 ..... **1**

1. INTRODUCTION **1**

1.1.PARKINSON'S DISEASE (PD) **1**

1.1.1. Incidence and Etiology **2**

1.1.2. Clinical Representation of Disease **2**

1.1.3. Genetic Background **3**

1.1.4. Role of alpha-synuclein in Disease Progression **5**

1.1.5. Hypothesis of Disease Emergence **7**

1.2. ZEBRAFISH (Danio Rerio) **9**

1.2.1. Strategies to develop transgenic zebrafish models **10**

1.2.2. Neurodegenerative disease modeling on zebrafish **13**

1.2.3. Parkinson's disease models on zebrafish **14**

1.3.AIM OF THE STUDY **17**

CHAPTER 2 ..... **19**

2. MATERIALS AND METHOD **19**

2.1. MATERIALS **19**

2.1.1. Cell Line **19**

2.1.2. Bacterial strains **19**

2.1.3. Plasmids **19**

2.1.4. Equipment and tools **20**

2.1.5. Chemicals and reagents **21**

2.1.6. Kits **23**

2.1.7. Enzymes **23**

2.1.8. Antibodies **24**

2.2. METHODS **25**

2.2.1. Buffers 25
2.2.2. Cloning of human alpha-synuclein (α-syn) 28
2.2.3. Zebrafish experiments 36
CHAPTER 3 41
3. RESULTS 41
3.1. Validation of amplified alpha-synuclein sequence 41
3.2. Cloning α-syn coding sequence to create middle entry clone 42
3.3. Validation of other plasmids 44
3.4. Final expression vector construction by gateway cloning and validation 45
3.5. In vitro transcription of transposase mRNA and validation 47
3.6. Transgenic zebrafish development and genotyping 48
3.7. Immunohistochemistry 49
CHAPTER 4 55
4. DISCUSSION 55
CHAPTER 5 55
5.CONCLUSION & FUTURE PERSPECTIVES 59
BIBLIOGRAPHY 61
APPENDIX 69

List of Figures

Figure 1.1.Different pathological outcomes of brain-first vs body-first PD. Adapted from Borghammer P., 2019 [49]. 8

Figure 1.2. Tol2 transposon-mediated transgenic development workflow 12

Figure 1.3.Structural differences between human and zebrafish synucleins. Adapted from Milanese et. al, 2012 [105] 16

Figure 2.1. Human alpha-synuclein open reading frame that codes for protein NM_000345.4 30

Figure 2.2. Final α-syn expression construct development using Multisite gateway cloning... 34

Figure 3.1.PCR products of α-syn visualized after agarose gel electrophoresis. **1-2-3:** products from different cDNA samples, **NT:** no template control. Bioline HyperLadder 1kb was used as a reference. 41

Figure 3.2. Validation of purified PCR products with Sanger sequencing. Sequencing data was checked with FinchTV for read quality, then aligned with human α-syn coding sequence using BLASTn. 42

Figure 3.3. **a)** PCR products of α-syn after adding cut sites to each end. **b)** Double digestion (KpnI- SmaI) product of pME-MCS vector. 43

Figure 3.4. Validation of pME-asyn plasmid after miniprep with single restriction digestion with ApaI enzyme. Lanes 1,12: Ladder, Lane 2: backbone without ligation (2765 bp), Lane 3,4,5,6: correct clones (3032 bp), Lanes 7,8,9,10,11: wrong clones digestion with ApaI enzyme. Lanes 1,12: Ladder, Lane 2: backbone without ligation (2765 bp), Lane 3,4,5,6: correct clones (3032 bp), Lanes 7,8,9,10,11: wrong clones 44

Figure 3.5..Representative map of pME-α-syn after sequencing 44

Figure 3.6. Representative plasmid maps of other plasmids according to sequencing data. Drawn in Benchling. 45

Figure 3.7.Validation mCherry sequence via colony PCR after LR recombination on agarose gel. The expected band size was 1690 bp. Three clones marked with red square are

correct since they gave the right size. 46

Figure 3.8. Validation of α-syn sequence via colony PCR after LR recombination on agarose gel. The expected band size was 423 bp. Three clones marked with red are positive, and these colonies gave both the right size mCherry and α-syn PCR products. 46

Figure 3.9. The final expression vector map was drawn according to the sequencing of the plasmid product using Benchling. 47

Figure 3.10. Transposase mRNA that was obtained after in vitro transcription. In the presence and absence of the DNase I enzyme, the integrity of the mRNA was observed. Target mRNA length was observed at the expected size of around 1000 bp. Hyperladder 1 kb DNA ladder was used as a reference. 48

Figure 3.11. Genotyping of zebrafish for alpha-synuclein presence. PCR products (423bp) were loaded on agarose gel and ran for 40 min at 90V. Bioline HyperLadder 1kb was used. .. 49

Figure 3.12. α-syn fibril presence in old zebrafish (2yo) after 1-h post-CVMI injection. Green: α-syn, Blue: DAPI, red: synaptophysin. Scale bar: 100µm..... 50

Figure 3.13. α-syn fibril presence in old zebrafish (2yo) after one-week post-CVMI injection. Green: α-syn, Blue: DAPI, red: beta-tubulin. Scale bar: 100µm..... 51

Figure 3.14. α-syn fibril presence in young (3 mo) zebrafish after a) 1h post-injection and b) 1-week post-injection to the brain. Blue: DAPI, Green: α-syn, red: beta-actin. Scale bar: 50 µm 52

Figure 3.15. α-syn fibril presence in gut of old (2 yo) zebrafish after 1-week post-injection to the brain. Blue: DAPI, Green: α-syn, red: beta-actin. Scale bar: 50 µm 53

Figure 3.16. α-syn fibril presence in a) brain and b) gut of young (3 mo) zebrafish after 1-week post-injection intraperitoneally. Blue: DAPI, Green: α-syn, red: beta-actin. Scale bar: 50 µm, 100 µm respectively. 54

List of Tables

Table 2.1. List of bacterial strains used 19

Table 2.2. List of plasmids that are used 19

Table 2.3.List of equipments 20

Table 2.4. List of biological materials, chemicals, antibiotics, and reagents used in this study 21

Table 2.5. Kits used in this study 23

Table 2.6. Enzymes used in this study 23

Table 2.7. Antibodies used in the study 24

Table 2.8. Colony PCR primers used in this study 33

CHAPTER 1

1. INTRODUCTION

1.1. Parkinson’s Disease (PD)

Parkinson's Disease (PD) is a neurodegenerative disease condition primarily attributed to the degeneration of dopaminergic neurons located in the central nervous system. Initially believed to manifest as motor disturbances primarily, it is now recognized to encompass an array of non-motor symptoms, including memory disturbances, gait dysfunction, sleep behavior problems, depression, and loss of smell. These additional symptoms notably augment the overall impact of the disease.[1].

PD profoundly affects society due to its widespread prevalence, with the incidence and prevalence rates sharply rising over the decades for reasons not yet fully elucidated. On an individual level, Parkinson's disease lasts for a long time and has a significant impact. It usually gets worse slowly and leads to increasing disability. Caregivers often face significant challenges because of the demands of the disease. Together, Parkinson's disease creates a growing economic burden.[2].

The primary indicators of PD become apparent when neurons in the basal ganglia degenerate, affecting a vital brain region responsible for motor control. These neurons

play a role in producing dopamine, a vital neurotransmitter that regulates motor function. As a result, the loss or dysfunction of these neurons leads to reduced dopamine production, causing the characteristic motor symptoms of PD [1].

1.1.1. Incidence and Etiology

The global incidence of Parkinson's disease is defined around 35 cases per 100,000 individuals annually [2]. Age is the primary risk factor for PD, with symptoms usually starting around age 65. The incidence increases with age, peaking in individuals aged 70 to 79. Prevalence rates vary by region, with higher frequencies in Europe and America and lower rates in Africa, Asia, and the Middle East.[3]. Incidence is also related to the country's industrialization [4]. Another factor affecting the prevalence of PD is defined as gender, whereas men have a higher risk than women because of the protective effects of estrogen [5]. As seen in many diseases, lifestyle is another important factor that can cause the disease occurrence. However, smokers and caffeine consumers are stated to have low risk to develope PD because the antagonistic effects of these chemicals on related receptors may cause neuroprotective effects [6], [7].

1.1.2. Clinical Representation of Disease

Clinical representation of Parkinson’s disease includes both motor symptoms such as bradykinesia, tremor, and postural instability, as well as nonmotor symptoms like psychotic symptoms, sleep behavior disorders, memory dysfunction, and depression [8]. Initial motor symptoms generally start years later than the disease begins. In terms of the manifestation of symptoms, PD is defined in three stages: preclinical, prodromal, and clinical [9]. At a preclinical stage, dopaminergic neuron loss has already been started.

Non-motor symptoms of Parkinson's disease typically manifest in the early stages of the condition. Interestingly, motor and non-motor symptoms often overlap in certain disease stages [10]. It is unlikely that clinically defined PD subtypes are distinctive; instead, they likely represent typical phenotypes within a varying spectrum resulting from different contributing factors [11]. An intriguing observation is the frequent association of axial motor symptoms, such as gait disturbances and sleep problems, with cognitive impairments, indicating the involvement of overlapping functional brain circuits [12]. Parkinson's disease (PD) is defined by protein inclusions called Lewy bodies in the dopaminergic neurons [13]. However, the progression of the disease may start in peripheral structures, spreading towards the brain. This also explains us the reason for potential early autonomic disturbances and hyposmia presence, which is highly prevalent [14]. In late stages, the telencephalic cortex, which is the brain region responsible for memory and mood is affected [11].

1.1.3. Genetic Background

Parkinson's disease has a genetic component, with some patients having specific rare genetic variants that cause familial disease, while others have a genetic predisposition based on standard risk variants [15]. Although the heritability of the disease is relatively low, both genetic and environmental factors likely play a significant role in causing Parkinson's disease [16].

PD forms are caused by a single gene mutation called monogenic forms. Research on PD genetics has been associated with six central genes: alpha-synuclein, VPS35, LRRK2, PINK1, DJ-1, and Parkin [17]. These genes are either defined as autosomal dominant or recessive according and defined in inheritance mode of familial PD [18]. Among these

six genes, alpha-synuclein (SNCA) and LRRK2 are found to play a role in familial PD development and causative factors for sporadic disease progression [19]. SNCA mutations were the first target identified in familial PD patients; even though their prevalence is rare for familial PD, mutated SNCA products cause rapid progression of the disease at comparably earlier ages (<50) than other disease-causing genes [20].

Leucine-rich repeat kinase 2 (LRRK2) is known as one of the causes of late autosomal and sporadic PD, and the disease's progression is slower than SNCA. LRRK2 has kinase and GTPase domains which are important in enzymatic kinase function. Pathogenic mutations of LRRK2 are mainly related to the mutation in enzymatic domains [21]. Unlike SNCA, clinical pathology of LRRK2-dependent PD does not show dementia in most cases [22]. It is reported that patients who have LRRK2 mutations also govern alpha-synuclein neuropathology as Lewy bodies [23].

Vacuolar protein sorting 35 (VPS35) mutations in late-onset autosomal dominant PD were first defined in 2011, reported in a Swiss family. This form is characterized by slow progression, with a high rate of tremors, and responsive to dopa [24]. VPS35 protein is a retromer complex that facilitates the transport between endosomes, Golgi, and lysosome [25]. Defects in the VPS35 are also associated with defective alpha-synuclein degradation because of the failure in lysosomal transport [26].

Parkin functions as a ubiquitin E3 protein-ligase and is also defined as one of the disease-causing genes for autosomal recessive PD [27]. Mutations in Parkin are also thought to have a role in sporadic PD, resulting in dopaminergic stress due to loss of E3 ligase function, which eventually causes neurodegeneration [28].

PTEN-induced putative kinase 1 (PINK1) is responsible for encoding a serine-threonine protein kinase that is mainly found in mitochondria. As a result, this protein kinase plays

a key role in regulating mitochondria and promoting the survival of neurons in the presence of oxidative stress. Additionally, mutations in PINK1 are a common cause of early-onset autosomal Parkinson's disease [29].

Protein deglycase DJ-1 is a small protein related to rare inherited forms [30]. It is extensively present in astrocytes and plays a role in various cellular functions, including apoptosis, the inflammatory response, and oxidative stress [31].

1.1.4. Role of alpha-synuclein in Disease Progression

Alpha-synuclein (α-syn) is a small (14 kDa), soluble protein mainly expressed in the CNS, PNS, and other tissues in the body [32]. α-syn has been considered naturally present in monomer form. However, recent research has uncovered that the majority of natural α-syn can also exist in tetramer form which is 58 kDa and demonstrates minimal or no tendency for aggregation [33]. Both tetrameric and monomeric forms are present, but disturbances in their ratio may result in increased forms that promote aggregation [34].

Alpha-synuclein (α-syn) comprises three primary domains: a lysine-rich N-terminus, a hydrophobic component that is non-amyloid, and C-terminus binding domain [35]. The N-terminus of the protein consists of four repeated sequences, which are involved in mitochondrial localization [36]. The non-amyloid component is associated with post-translational modifications and alterations in secondary structure [35]. Lastly, the C-terminal segment modulates nuclear localization. Misfolding of α-synuclein leads to insoluble fibrils accumulating primarily within neurons [37].

Mutant α-syn proteins differ by only a few amino acids, yet these small changes lead to significant alterations in their conformation and the types of aggregates they form [38].

Mutant α-syn forms linked with Parkinson's disease, specifically the A30P and A53T mutations [39], have been shown to have structural defects that affect binding to cell membranes and change the protein's characteristics for the ability to bind [40].

The transneuronal propagation of alpha-synuclein (α-syn) plays a pivotal role in shaping the course of Parkinson's disease (PD), significantly influencing its development and progression. The transmission of pathological α-syn pathways occurs via cell-to-cell or synaptic means [41]. Notably, in vivo, α-syn aggregates spread akin to prions, with distinct conformations functioning as seeds that neighboring cells internalize. Consequently, this process induces the misfolding of protein and structural disruption of normal α-syn [42].

In the prodromal stage of PD, the initial phase of neurodegeneration is characterized by a significant decline in the survival of neurons. During this period, non-motor symptoms become evident, accompanied by markers of neurodegeneration and a notable rise in peripheral inflammatory markers [43]. Subsequently, there is a surge in inflammatory markers, followed by a gradual decline during the early motor stage [44]. Throughout the prodromal and early motor stages, there is a sustained elevation in the ratio of oligomeric α-syn compared to total α-syn. Assessing early α-synuclein aggregates may facilitate early PD detection, as the α-synuclein oligomerization results in the death of neurons under disease conditions [45]. Consequently, α-synuclein-related biomarkers present a unique opportunity for therapeutic intervention before significant dopaminergic denervation [46].

Preformed fibril (PFF) models replicate both pathological and behavioral aspects of synucleinopathies. The spread of aggregates in PFF models depends on the seed type. Regardless, PFFs lead to progressive protein aggregation, neuronal loss,

neuroinflammation, and behavioral changes. These pathological changes can result from the gradual accumulation of α-syn proteins by a small injection of similar aggregates. PFF models offer advantages over existing models, making them valuable for studying disease development and designing treatments [41].

Currently, there are no disease-modifying therapies for α-syn pathology. New approaches are needed to reduce protein levels, inhibit the misfolding of proteins that result in aggregation, and modify post-translational processes.

1.1.5. Hypothesis of Disease Emergence

In the Braak staging system, α-synuclein pathology first appears in the dorsal motor nucleus in the brain and also the olfactory bulb, possibly due to damage to the enteric and olfactory epithelium. [13]. However, it is noteworthy that the Braak staging system does not universally apply to all cases of Lewy pathology at post-mortem, with particular instances exhibiting no pathology despite featuring pathology in higher-stage, such as the substantia nigra [47], [48].

In addressing this controversy, a recent hypothesis proposes that Parkinson's disease (PD) may encompass two subtypes: brain-first PD and body-first PD [49]. Brain-first PD represents the subtype wherein α-synuclein pathology initially arises in the brain and disseminates through the spinal cord and enteric nervous system. Conversely, body-first PD signifies the subtype in which α-synuclein pathology initiates in the enteric nervous system, travel to the lower brain regions, eventually to the entire brain [50].

Brain-first and body-first Parkinson's disease (PD) may possess two distinct phenotypes based on specific pathological and imaging markers. Patients with body-first PD tend to experience a greater degree of autonomic symptoms, especially constipation, and show cardiac dysfunction. In prodromal stages, body-first patients also highly display REM

sleep behavior disorders [51]. Magnetic resonance imaging (MRI) studies have identified structural changes in brain, including significant damage to the locus coeruleus, in body-first PD patients. Body-first PD patients also have a higher rate of α-synuclein presence in the intestine and also in the skin. Imaging of dopamine levels indicates that degeneration in brain-first PD accumulates asymmetrically, which correlates with the motor symptoms seen in this subtype. Additionally, pathological genes causing PD often show the features of the brain-first subtype, while others are more aligned with the clinical profile of body-first PD [52].

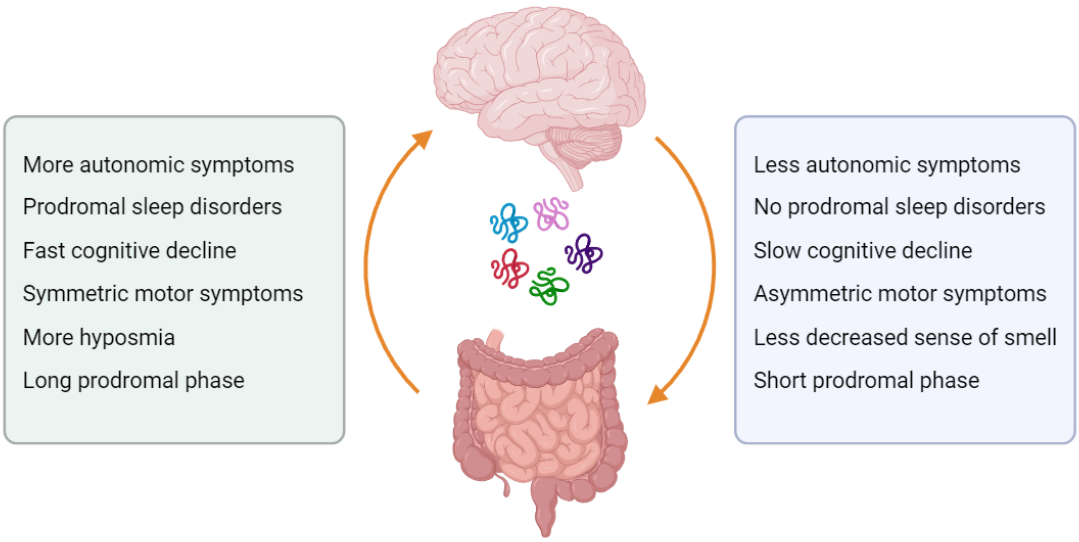

Figure 1.1.Different pathological outcomes of brain-first vs body-first PD. Adapted from Borghammer P., 2019 [49].

1.2. Zebrafish (*Danio Rerio*)

Zebrafish (*Danio rerio*) are small tropical freshwater fish in Asia, specifically India [53]. They have been discovered and used extensively as model organisms for many human diseases. In laboratory conditions, they are maintained as groups in 3.5 or 8 liters tanks at a temperature between 26-28°C with lighting conditions of 14h:10h. (light:dark) [54]. Their advantageous features allow them to model many conditions, including developmental, mental, infectious, and metabolic human diseases [55].

Firstly, compared to rodent models, zebrafish are easy to handle and generate large number of offspring (50-300 eggs) in a single breeding [56]. During early developmental stages, the larvae's optical clarity provides a significant advantage with direct live imaging of the whole organism [57]. Zebrafish have comparable organs to humans, including eyes, mouth, brain, spinal cord, heart, intestine, liver, kidney, blood, cartilage, and teeth [58]. The life cycle of zebrafish is approximately two years. On day three, it hatches from the egg; on day 21, it becomes a juvenile after metamorphosis. It reaches sexual maturity at three months old and is considered an adult [59]. This feature makes zebrafish a valuable model for aging studies with comparable aging-related cellular and neurological changes [60]. Zebrafish are sexually dimorphic. Therefore, sex-dependent differences can be monitored easily [61].

Zebrafish are also an efficient model for studying behavioral changes such as anxiety, aggression, learning, memory, and social interaction, both in larval and adult stages [62] [63].

The zebrafish genome is completely known and sequenced up to now, and it shows 70% homology to the human genome [64]. Moreover, 80% of human disease-related proteins are conserved in zebrafish [65].

Since zebrafish share similarities with humans, diseases studied in zebrafish often serve as reliable models of human diseases. These models accurately reflect the diseases' causes, development, and resolution. Through precise gene editing in zebrafish, we can create models that mimic certain disease-causing genetic variations found in human patients [66].

1.2.1. Strategies to develop transgenic zebrafish models

Transgenesis is a vital method for investigating biological processes in living organisms which facilitates live imaging, lineage tracing, mutant creation, and disease modeling experiments. Transgenic lines make it possible to label cells, model diseases, and create mutations, making transgenesis an indispensable tool for studying developmental processes [67]. The benefits of using zebrafish for gene editing compared to other species are numerous, including a high fecundity, external fertilization, straightforward injection process, and easy genotyping. However, a significant difficulty arises from early-stage embryos' rapid development and division, necessitating a short gene editing timeframe and an mRNA and protein-based editing system to enhance effectiveness [68].

One commonly utilized technique for disrupting genes' function in zebrafish is the introduction of short antisense oligonucleotides, known as morpholinos, into early embryos. This targeted approach reduces the gene expression of interest, leading to the emergence of related traits. Depending on the specific target sequence, the morpholinos block the expression of the corresponding RNA, which results in diminished or no gene product expression. This technique is a powerful tool in zebrafish research, providing a clear understanding of gene function and its potential role in disease [69].

The overexpression of mRNA is a useful technique for comprehensive gene analysis. However, due to the instability of injected mRNA, its effects can only be observed during early embryonic stages. This method is also employed to confirm loss-of-function traits through giving wild-type mRNA to rescue function. [70].

Mutations can be targeted in zebrafish through various methods. Zinc finger nucleases (ZFNs) are endonucleases that target specific DNA sequences present in the genome. When targeted, ZFNs form a dimer that enables to cutting of double-stranded DNA, resulting in double-strand break (DSB) [71]. Transcription activator-like effector nucleases (TALENs) comprise repeats that are mostly conserved in the binding region of DNA and only show variation at two sites that affect binding specificity. Like ZFNs, TALENs are also able to bind specifically to the target and enable the introduction of a double-strand break [72]. The CRISPR-Cas9 system, which is a highly popular mechanism, depends on the delivery of both an endonuclease called Cas9 and a guide RNA specifically targeting the region on the genome. Cas9 has the ability to recognize targets with the help of guide RNA. Then, it introduces a double-strand break [73]. In genome editing, there are certain drawbacks, such as off-target effect, which can result in unwanted mutations. Therefore target genomic sequences should be unique and chosen wisely to minimize the off-target effects. Additionally, only small sequences can be inserted when creating knock-ins or novel inserts [74].

To create stable transgenes reliably, it is necessary to integrate the respective construct into the zebrafish genome actively. Various transposon-related tools are available for zebrafish, including Sleeping Beauty and Tol2, with Tol2 being the most popular because of function ease and efficiency in facilitating easy integration into the genome [70] [71]. Tol2-based transgenesis involves delivering transposase mRNA and an expression vector

containing the desired transgene inserted between two Tol2 transposon repeats to provide random insertions to the target genome effectively. This approach is well-suited for use in zebrafish, which entails the one-cell stage injection of transposase mRNA and a target cassette containing transgenesis plasmid [77]. The activity of Tol2 transposon for transgenesis has also been successfully used in other species like chickens, Xenopus, and killifish by using different delivery methods such as injection or electroporation [78]. The transposase can be provided on a separate DNA expression cassette in trans or outside of the transposon cassette. However, in zebrafish, transposase is often supplied is supplied by co-injection of mRNA that encodes the transposase, ensuring transient availability and stable transposon integrations following natural mRNA degradation [79]. Numerous zebrafish transgenesis vectors incorporate a reporter cassette for quality control and subsequent work during transgenesis. It is crucial to verify that transposition occurs in the embryos for successful transgenic fish production. This quality control assessment can be efficiently conducted when the expression plasmid contains a fluorescent marker such as EGFP, mCherry, and dsRed. [80].

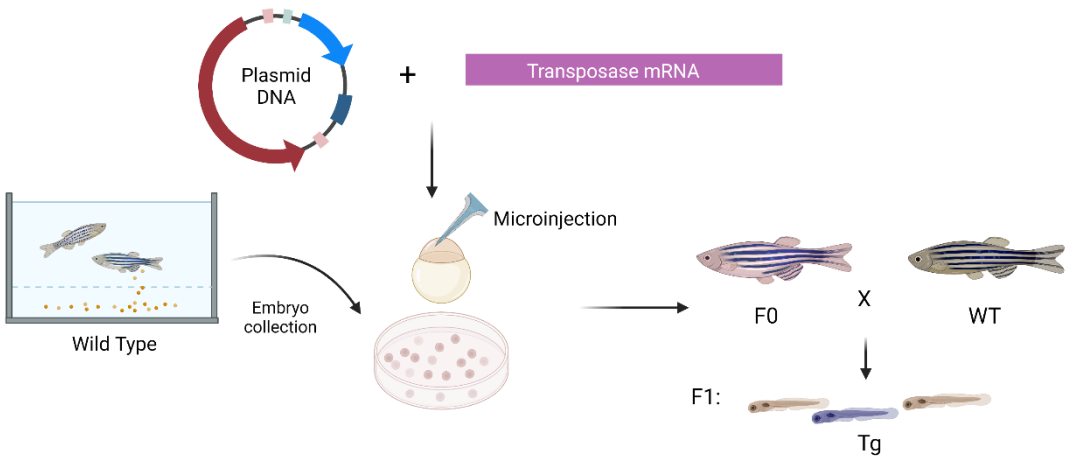

Figure 1.2. Tol2 transposon-mediated transgenic development workflow

The Tol2 toolbox is also useful for researching neurodegenerative disorders in zebrafish. It can encompass promoters for specific cell types, such as astrocytes, cortical neurons, microglia, and many others along with various fluorescent proteins as markers. This toolbox allows for the insertion of genes of interest or disease-related genes, aiming to accelerate the adaptable creation of zebrafish models to explore the CNS function and the disease mechanisms leading to neurodegeneration [81].

1.2.2. Neurodegenerative disease modeling on zebrafish

Despite differences in the organization of the central nervous system, the zebrafish brain shares many similarities with mammals, including several cerebral nuclei like the basal ganglia, striatum, hippocampus, and amygdala [82]. The zebrafish neurotransmitter system shows high similarity to mammals starting from early development, such as the population of dopaminergic cells in different brain regions and the ability to produce neurotransmitters similar to humans such as dopamine, serotonin and GABA [83].

Zebrafish provides a viable approach for modeling neurodegenerative diseases due to its advanced imaging technologies, comparable behavioral testing, and high-throughput drug screening capabilities. Numerous models are available for neurodegenerative diseases including Alzheimer's disease (AD) [84], Parkinson's disease (PD) [85], and Amyotrophic lateral sclerosis (ALS) [86]. These models are developed through genetic manipulations (transient/stable) or chemicals and neurotoxins [87].

As an example of chemical-induced models, Okadaic acid (OKA), which is an inhibitor of protein phosphatase 2A (PP2A), is extensively used to develop the AD zebrafish model. In these models, amyloid aggregation, plaque formation, and increased phosphorylated tau were visible in the brain of the zebrafish [88], [89]. Genetic

manipulations for developing Alzheimer's disease (AD) models in zebrafish are also widely favored. Mutant APP, which results in abnormal amyloid-beta formation, is associated with familial form of AD, and zebrafish possess genes that are analogous to those found in humans [90]. In mutant APP zebrafish, protein that causes the disease is expressed in many organs such as brain, eyes, vascular system and heart. This presented model demonstrates behavioral symptoms that observed in AD patients, β-amyloidosis, and neuronal loss [91].

In the case of Amyotrophic Lateral Sclerosis (ALS), alterations in the superoxide dismutase 1 (SOD1) gene have been found to impact various aspects of zebrafish motor neuron function, such as outgrowth, axonal branching, neuromuscular junction integrity, and survival [92]. Additionally, zebrafish models with mutated TDP43, a nuclear protein associated with ALS progression, exhibit motor dysfunction and anomalies in motor axon development [93].

1.2.3. Parkinson’s disease models on zebrafish

Like other neurodegenerative conditions, Parkinson's disease can be replicated through chemical induction or genetic manipulations. In zebrafish, the main inducers of a Parkinson's disease-like phenotype are 1-methyl-4-phenyl-1,2,3,6-tetrahydropyridine (MPTP), 6-hydroxydopamine (6-OHDA), rotenone, and paraquat. MPTP has been shown to cause loss of dopaminergic neurons in the diencephalon of both adult [94] and larval fish [95], resulting in locomotor defects, reduced dopamine levels, and reduction in mitochondrial transport [96], [97]. 6-OHDA administration to zebrafish causes a reduction of TH-positive neurons, decreases dopamine levels, and abnormalities in

locomotor function [98], [99]. Similarly, exposure to rotenone and paraquat shows abnormalities in behavior, learning, and motor functions [100], [101]. Although these chemically induced models represent great potential, it is solely dependent on concentration, and results are highly variable. It is still beneficial to screen high-throughput compound libraries for neuroprotection against resulting disease-related pathological changes.

Zebrafish models that are based on genetic changes have been widely employed to enlighten the pathology of Parkinson's disease (PD) and find potential therapies. Zebrafish have a gene homologous to the human LRRK2 gene, and disrupting it causes developmental defects and neuron loss [102]. However, studies need to show consistent results. Therefore, a zebrafish model for increased LRRK2 kinase activity relevant to Parkinson's disease has not been created yet [85]. Reducing parkin activity in zebrafish is shown to result in less presence of dopaminergic neurons. In addition, the knockdown of the parkin gene in zebrafish shows specific impairments in mitochondrial function [103]. Knock-down of PINK1 also results in the reduced number of dopaminergic neurons in zebrafish. When taken together with other PD-causing factors, these models can effectively replicate PD pathology by causing mitochondrial dysfunction and loss of dopaminergic neurons [104].

Despite lacking a gene equivalent to human alpha-synuclein (α-syn), zebrafish do possess analogous genes known as beta-synuclein (β-syn), gamma1-synuclein (γ1-syn), and gamma2-synuclein (γ2-syn). Of these, γ1-synuclein has been shown to have a similar role to α-synuclein. Reduction in the expression of β- and γ1-synucleins are shown to result in developmental defects of dopaminergic neurons, eventually leading to a

decrease in dopamine levels [105].

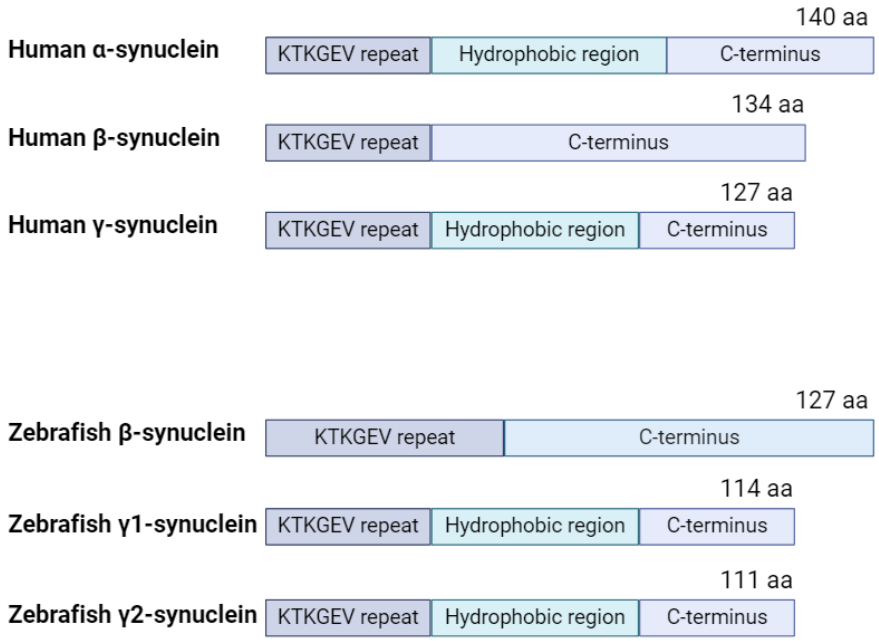

Figure 1.3.Structural differences between human and zebrafish synucleins. Adapted from Milanese et al., 2012 [105]

A study revealed that inadequate expression of human α-synuclein can elevate the cytoplasmic flux of peroxides and lead to oxidative stress. This condition results in abnormalities in motor function and then leads to the loss of neurons [106]. Recent zebrafish models expressing human α-synuclein demonstrated that it induces extensive protein aggregation, disruptions of functioning mitochondria in axons, and cell death. However, these models only focus on expression in a subset of neurons in CNS [107], [108]. Despite being a promising candidate for modifying Parkinson's disease, current zebrafish models of PD only exhibit a phenotype involving the dopaminergic neuron loss without showing the formation of Lewy bodies.

1.3. Aim of the study

Based on our comprehensive literature review, zebrafish emerges as a promising model organism for studying neurodegenerative diseases. While the emergence and progression of alpha-synuclein pathology in these diseases is not yet fully understood, zebrafish have the potential to bridge this gap. The brain-first and gut-first hypotheses, previously described from pathological samples and scans of human patients, provide a starting point. However, the initial emergence and changes in different body regions cannot be fully understood without a suitable model organism, which zebrafish could potentially provide.

Given that zebrafish do not naturally express homologous alpha-synuclein, the creation of a new model that closely mimics human conditions is not just important, but imperative for a comprehensive understanding of disease pathology. This urgency underscores the significance of our research.

For this purpose, this research focuses on developing a new transgenic model to further study the function of alpha-synuclein and the progression of diseases depending on whether fibrillation starts within the brain or gut. Although transgenic zebrafish are available for modeling Parkinson's disease, these only focus on small subsets of neurons in the brain. Therefore, they are limited to providing additional information about how alpha-synuclein aggregation and Lewy body pathology progresses between the gut and the brain. In our model, by choosing a universal promoter specific to neurons and other parts of the zebrafish body, we aimed to observe the expression of human alpha-synuclein, at least at basal levels. To achieve this, an extensively used method called gateway cloning and Tol2 transgenesis was used to produce a target expression vector that can integrate the zebrafish genome. This expression is aimed to be followed across

generations since transposase stably integrates the target sequence into the genome. We also aimed to observe that alpha-synuclein fibrils could still spread to zebrafish brains or gut by performing fibril injections on wild-type fish. To follow the fibril behavior, injections of the gut and brain were performed on both young and old fish, and how retainment of fibrils after injection changes due to aging.

Our objective is to develop diverse models that can express various types of alpha-synuclein mutants in zebrafish. This endeavor aims to gain a deeper understanding of the mutant forms and their influence on the progression of pathology in the future.

CHAPTER 2

2. MATERIALS AND METHOD

2.1. Materials

2.1.1. Cell Line

HMC3 (Human microglial cell line), ATCC CRL-3304, Passage < 30

2.1.2. Bacterial strains

Table 2.1. List of bacterial strains used

Strain Name	**Catalog Number**	**Brand**
Escherichia coli JM109	L2005	Promega
Escherichia coli ccdb-resistant bacteria	A10460	Invitrogen
Escherichia coli DH5-alpha	T3007	Zymo Research

2.1.3. Plasmids

Table 2.2. List of plasmids that are used

Plasmid Name	**Insert**	**Resistance**	**Type**	**Size**
pENTR5'_Ubi	Zebrafish ubiquitin promoter	Kanamycin	Entry	2692 bp
pME-MCS	Multiple cloning site from	Kanamycin	Entry	2765 bp

	BlueScript			
p3E-mCherrypA	mCherry with SP40 late polyA	Kanamycin	Entry	3586 bp
pDONR221	Middle donor vector	Kanamycin/chloramphenicol	Donor	4761 bp
pDEST	Destination vector with attR4-R3	Ampicillin/chloramphenicol	Destination	7796 bp
pCS2FA-transposase	Capped Tol2 transposase	Ampicillin	Expression	6034 bp

2.1.4. Equipment and tools

Table 2.3. List of equipments

Equipment	**Catalog Number**	**Brand**
16 mm coverslip	SUP0111600	Marienfeld
Benchtop Centrifuge	CT6E	VWR
ChemiDoc MP Imaging System	Universal Hood III	Bio-rad
CO2 Incubator	CCL-170B-8	ESCO
Confocal Microscope	SP8 Confocal Microscope	Leica
Cooling Centrifuge	CT15RE	VWR
Cryostat	CM1850	Leica
Electrophoretic Gel System	EC370M	E-C
Hemocytometer	0640110	Marienfeld-Neubauer
HistoBond adhesive microscope slides	0810001	Marienfeld
Incubator	INCU-Line	VWR
Inverted Microscope	Axio Observer A1	Zeiss
Laminar Flow	Class II Safety Cabinet	Metisafe
Mini centrifuge	Centrifuge 5418	Eppendorf
Mr. Frosty Freezing Container	5100-0001	Thermo Fisher Scientific
Otoclave	SteamArt OT 90L	Nüve

Ph Meter	SevenCompact	Mettler Toledo
Power Supply	PowerPac Basic	Bio-rad
Rattler Plating Beads	S1001	Zymo Research
PAP Pen	ab2601	Abcam
Rocker	Nutating Mixer	VWR
Shaker	VMS-C4 Advanced	VWR
Shaker Incubator	Innova 44	New Brunswick Scientific
Thermal Cycler	C1000 Thermal Cycler	Bio-rad
Vortex	Vortex Mixer	VWR
Waterbath	Bath NB9	Nüve
Laboratory scale	BJ410C	Precisa
Zebrafish Breeding Tank	-	Custom-made
Syringe Pump	NE300	New Era Pump Systems
Insulin Syringe 1cc	P36139.001	Beyanlab
Microloader Pipette Tips	10289651	Eppendorf
Glass Capillary Needles	BF100-50-7.5	Sutter Instruments
Micropipette Puller	P-30	Sutter Instruments
Hamilton 10 µl Microliter Syringe Model	80301	Hamilton

2.1.5. Chemicals and reagents

Table 2.4. List of biological materials, chemicals, antibiotics, and reagents used in this study

Cell Culture		
Product	**Catalog Number**	**Brand**
Dimethyl Sulfoxide (DMSO)	F-515	Thermo Fisher Scientific
Fetal Bovine Serum (FBS)	S-FBSP-EU-015	Serana
MEM Eagle Non-Essential Amino	01-340-1A	Sartorius

Acids Solution X100 (NEAA)		
Minimum Essential Media with Earle's Salts and with L-glutamine	MCL-052-500ML	Serana
Penicillin-Streptomycin (P/S)	L0022-100	Biowest
Trypsin 0.25% - EDTA 0.02% in HBSS (Trypsin-EDTA)	L0932-100	Biowest
Dulbecco's Phosphate-buffered saline (DPBS)	D8537-500ML	Sigma-Aldrich
Trypan Blue	T8154-100ML	Sigma-Aldrich
Biological Materials		
Product	**Catalog Number**	**Brand**
Healthy Brain RNA-cDNA	R1234035-P	Biochain
Chemicals		
Product	**Catalog Number**	**Brand**
Agar	05039-500G	Sigma-Aldrich
Peptone	1616.00	Condalab
Sodium Chloride (NaCl)	969.033.1000-1KG	Isolab
Tryptone	1612.00	Condalab
Yeast Extract	92144-500G-F	Sigma-Aldrich
Potassium Chloride	960.033	Interlab
Calcium chloride dihydrate	102382	Merck
Magnesium sulfate heptahydrate	M1880	Sigma-Aldrich
Methylene Blue	947.D05	Interlab
5x DNA Loading Buffer Blue	BIO-37045	Bioline
Agarose Tablets	BIO-41027	Bioline
Ampicillin Sodium Salt	A9518-5G	Sigma-Aldrich
Acetic Acid	901.013.2500	Merck
Hydrochloric acid	932.103	Interlab
Chloramphenicol	16785.03	Serva
Calcium chloride dihydrate	12022-1KG	Sigms-Aldrich
HyperLadder 1kb	H1-617112A	Bioline
Kanamycin Sulfate – H2O	26899.02	Serva

Nuclease Free Water	P119E	Promega
SYBR Safe DNA gel stain	S33102	Invitrogen
Methanol	32213-2.5L	Sigma-Aldrich
4′,6-diamidino-2-phenylindihydrochloride (DAPI)	D9542-1MG	Sigma-Aldrich
Formaldehyde 37%	1.04002.2500	Merck
Bovine Serum Albumin	P6155	Biowest
Isopropanol	109634	Merck
Trizma base	T1503-500G	Sigma-Aldrich
Sucrose	S0389	Merck
Triton X-100	T8787	Sigma-Aldrich
Optimum Cutting Temperature (O.C.T.)	4583	Tissue-Tek

2.1.6. Kits

Table 2.5. Kits used in this study

Kit	**Catalog Number**	**Brand**
Direct-zol RNA Miniprep	R2050	Zymo Research
Expin Combo GP mini	112-150	GeneAll
NucleoSpin Plasmid, mini kit for plasmid DNA	740588.50	Macherey Nagel
ZymoPURE II Plasmid Maxiprep Kit	D4202	Zymo Research
mMessage mMachine SP6 Transcription Kit	AM1340	Thermofisher Scientific

2.1.7. Enzymes

Table 2.6. Enzymes used in this study

Enzyme	**Catalog Number**	**Brand**
HindIII-HF	R3104S	New England Biolabs (NEB)
KpnI-HF	R3142S	New England Biolabs

		(NEB)
SmaI	R0141	New England Biolabs
EcoRI-HF	R3101S	New England Biolabs (NEB)
NotI-HF	R3189S	New England Biolabs (NEB)
iScript Reverse Transcription Supermix for RT-qPCR	1708841	Bio-rad
Phusion High-Fidelity PCR Master Mix with HF Buffer	F531L	Thermo Scientific
Taq 2x Master Mix with 1,5 mM MgCl2 Red	A140301	Ampliqon
T4 DNA Ligase 5 Weiss U/ul	EL0011	Thermo Scientific
Gateway™ BP Clonase™ II Enzyme mix	11789020	Invitrogen
LR Clonase™ II Plus enzyme	12538120	Invitrogen

2.1.8. Antibodies

Table 2.7. Antibodies used in the study

Antibody	**Catalog Number**	**Brand**	**Dilution**
Alpha synuclein (Rabbit mAb)	E4U2F	Cell Signaling Technologies	1:400
Synaptophysin	ab309493	Abcam	1:400
Beta actin	ab170325	Abcam	1:800
Beta III tubulin	ab78078	Abcam	1:200
Cy5 AffiniPure™ Donkey Anti-Rabbit IgG (H+L)	711-175-152	Jackson Immuno Research	1:1000
Cy3 AffiniPure™ Goat Anti-Mouse IgG (H+L)	115-165-003	Jackson Immuno Research	1:1000

2.2. Methods

2.2.1. Buffers

10X TAE (stock):

48,5-gram Tris-base

11,4 ml Acetic Acid

20 ml 0,5M EDTA

Dissolved in 800 ml of distilled water. Then final volume was completed to 1 L.

1X TAE:

900 ml of distilled water is added to 100 ml of 10X stock solution.

0.5M EDTA:

168,1 gram EDTA disodium salt was dissolved in 800 ml of distilled water. pH was adjusted to 8.0 with HCl. The final volume was completed to 1 L.

Luria Broth (LB):

5-gram yeast extract

10-gram peptone

10-gram NaCl

12-gram Agar

Dissolved in 1 L of distilled water and autoclaved at 121°C at 15 psi for 15 minutes.

LB Agar:

After preparing the LB, as explained above, 7.5% agar was added to the final volume.

The solution was then autoclaved at 121°C at 15 psi.

1 M $CaCl_2$ (stock solution):

11,1 gram $CaCl_2$ anhydrous was weighed and dissolved in 80 ml of distilled water. Solution was mixed until fully dissolved, then volume is completed to 100 ml. Final solution was filter-sterilized through 0.22µm pore.

0.1M $CaCl_2$ solution:

10 ml of 1M $CaCl_2$ was added to 90 ml of distilled water (1:10). Final solution was filter-sterilized through 0.22µm pore.

HMC3 Complete medium:

5 ml Fetal Bovine Serum

500 µl non-essential amino acids

500 µl pen-strep

44 ml MEM with L-glutamine

Media was prepared under sterile conditions and stored at 4°C.

Cell Freezing Medium:

For stocking 1 vial of cells (1 ml): 100 µl DMSO and 900 µl Fetal Bovine Serum were mixed.

4% Paraformaldehyde:

40 grams of paraformaldehyde was dissolved in preheated 800 ml of sterile PBS solution. Once the solution was cooled, it was sterile-filtered and adjusted volume to 1L with PBS.

Sucrose solution:

To perform tissue dehydration, 10%, 20%, and 30% sucrose solutions were prepared

(w/v).

10% sucrose solution: 1 gram of sucrose was dissolved in 10 ml distilled water.

20% sucrose solution: 2 grams of sucrose was dissolved in 10 ml distilled water.

30% sucrose solution: 3 grams of sucrose was dissolved in 10 ml distilled water.

10X TBS solution (stock):

12 grams of Trizma Base

80 grams of NaCl

Dissolved in 800 ml of distilled water with magnetic stirrer. pH was adjusted to 7.6 with HCl. Final solution volume was completed to 1 L.

1X TBS solution:

100 ml of 10X TBS stock solution was mixed with 900 ml of distilled water.

TBS 0.025% Triton X-100 (TBS-T) solution:

250µl Triton X-100 was added to 1L 1X TBS.

Blocking (5% BSA in TBS-T) solution:

0.5 gram BSA was dissolved in 10 ml TBS-Triton solution.

Alpha-synuclein PFF preparation:

5mg/ml stock solution was diluted with sterile PBS and loading dye to have 10 µl of 1mg/ml final concentration of injection solution.

60X Embryo medium (E3):

17,2 grams of NaCl

0,76 grams of KCl

2,9 grams of $CaCl_2.2H_2O$

4,9 grams of $MgSO_4.7H_2O$

Dissolved in 800 ml of double distilled water. The volume was completed to 1L after completely dissolving. Final solution was autoclaved and stored at 4°C.

1X Embryo medium (E3):

16 ml 60X E3 medium was added to a glass bottle, and the volume was completed to 1L with distilled water. 10µl methylene blue was added to the final solution and stored in RT.

DNA Lysis Buffer:

Tris-HCl, pH=8.5, 50 mM

EDTA 1mM

Tween-20, 0.5%

Add 2 µl fresh Proteinase K 200µg/ml later.

2.2.2. Cloning of human alpha-synuclein (α-syn)

To clone human alpha-synuclein coding sequence (CDS) to target plasmid, isolation from cell culture was performed, and a human healthy brain cDNA sample was used.

2.2.2.1. Cell Culture

Stock HMC3 cell line was thawed in a water bath until partially dissolved, sterilized with 70% ethanol, and processed under a laminar flow hood. DMSO in the freezing medium of cells is toxic; therefore, before plating the cells, DMSO should be removed. Firstly, cells in the freezing medium were diluted by using the fresh complete medium in a 1:4 ratio. The mixture was placed in a 15 ml sterile falcon tube and centrifuged at 1500 rpm for 5 min to pellet the cells only. After centrifugation, the supernatant was discarded, and the cell pellet was gently resuspended with 7 ml fresh complete medium and plated to a T25 cell culture flask. In the following days, cells were constantly monitored for

attachment and confluency. Until cells reached the confluency, the medium was regularly changed to discard dead cells and waste metabolites. When confluency reached above 90%, cells were passaged using Trypsin-EDTA and incubated at 37°C incubator until detachment. Cells were checked under an inverted microscope; trypsin was inactivated with Fetal Bovine Serum (FBS) and split into 6-well plates with a seeding density of 10^5 cells/well.

2.2.2.2. Total RNA Isolation from HMC3 cells

After cells reached confluency ($1x10^6$ cells/well) in 6-well plates, an RNA isolation with RiboEx Trizol Reagent was performed according to the manufacturer's protocol. The medium was discarded, and cells were washed twice with sterile PBS. After discarding the PBS, 500µl RiboEX Trizol Reagent was added to each well, and cells were collected with a sterile cell scraper. Cells were incubated at room temperature for 5 min to allow complete homogenization. Then, 100µl chloroform was added to each sample, vortexed for 15 sec., and stored at room temperature for 2 min. Centrifugation at 12000 x g for 15 min at 4°C was performed, clear aqueous phase was transferred to a new 1.5ml tube without disturbing the mid layer. 250 µl isopropanol was added to the aqueous phase and gently mixed by inverting five times. Samples were incubated at room temperature for 10 min, then centrifuged at 12000 x g for 10 min at 4°C. Supernatant was discarded without disturbing the pellet. Pellets were washed using 1ml 75% ethanol. Last centrifugation was performed at room temperature at 7500 x g for 5 min. Remaining ethanol was carefully discarded, and pellets were air-dried under sterile conditions. Pellets were resuspended in 20µl of nuclease-free water and stored at -80°C until further usage.

2.2.2.3. Reverse transcription (RT) and cDNA synthesis

To perform cDNA synthesis, iScript Reverse Transcription Supermix was used and performed according to the manufacturer's protocol.

Component	Volume/reaction
iScript mix	4 µl
RNA template (200 ng/µl)	5 µl (1µg)
Nuclease-free water	11 µl
Total	20 µl

Reaction	Temperature	Time
Priming	25°C	5 min
RT reaction	46°C	20 min
Inactivation	95°C	1 min

2.2.2.4. Amplification of alpha-synuclein

The coding sequence of alpha-synuclein from human-derived cDNA samples was performed to express human alpha-synuclein in zebrafish. To this purpose, an alpha-synuclein primer pair without including the stop codon of the gene was designed according to the sequence obtained from NCBI NM_000345.4 (Figure 2.1).

Nucleotide Sequence (423 nt):

ATGGATGTATTCATGAAAGGACTTTCAAAGGCCAAGGAGGGAGTTGTGGCTGCTGCTGAGAAAACCAAAC
AGGGTGTGGCAGAAGCAGCAGGAAAGACAAAAGAGGGTGTTCTCTATGTAGGCTCCAAAACCAAGGAGGG
AGTGGTGCATGGTGTGGCAACAGTGGCTGAGAAGACCAAAGAGCAAGTGACAAATGTTGGAGGAGCAGTG
GTGACGGGTGTGACAGCAGTAGCCCAGAAGACAGTGGAGGGAGCAGGGAGCATTGCAGCAGCCACTGGCT
TTGTCAAAAAGGACCAGTTGGGCAAGAATGAAGAAGGAGCCCCACAGGAAGGAATTCTGGAAGATATGCC
TGTGGATCCTGACAATGAGGCTTATGAAATGCCTTCTGAGGAAGGGTATCAAGACTACGAACCTGAAGCC
TAA

Figure 2.1. Human alpha-synuclein open reading frame that codes for protein NM_000345.4

Primers:

Asyn-forward: CGACGACAGTGTGGTGTAAAG, GC:52.38%, T_m: 59.2°C

Asyn-reverse-nostop: GGCTTCAGGTTCGTAGTCT, GC:52.63%, T_m: 57°C

PCR conditions were performed as initial denaturation at 95°C degree for 5 min, 30 cycles of 95°C for 30 sec, 58°C for 30 sec, 72°C for 40 sec, and final elongation at 72°C for 5 min.

PCR products were run on 1% Agarose gel for 40 min at 90V. Bands were visualized under the ChemiDoc visualization system for validation. PCR products were then purified using a ComboGP mini kit by following the manufacturer's protocol to add cut sites and/or recombination sites.

2.2.2.5. Generation of middle entry clone containing α-syn

The pME-MCS vector was used as the backbone to generate the middle entry vector for gateway recombination later. This vector contains multiple restriction enzyme sites to integrate the target sequence. The integration of α-syn into the backbone vector was performed by a general cloning protocol with three steps: addition of cut sites to the PCR product, restriction digestion of the plasmid backbone, and α-syn PCR product to create overhangs and ligation.

The PCR product and pME-MCS vector were double digested using the enzymes KpnI (forward) and SmaI (reverse). For PCR products, the initial addition of cut sites was performed as follows.

Asyn-KpnI forward: ATTAATGGTACCACGACAGTGTGGTGT, Tm: 65°C

Asyn-SmaI reverse: AATTCGCCCGGGGGCTTCAGGTTCGTAGTCT, Tm: 70°C

PCR reaction was performed as initial denaturation at 95°C for 5 min, then 30 cycles of 95°C for 30 sec, 69°C for 30 sec, 72°C for 40 sec, and 72°C for 5 min for final elongation.

After the PCR reaction, PCR products were run and visualized using agarose gel, and the final product was purified with Expin Combo GP kit protocol.

Double digestion with KpnI and SmaI was performed according to the manufacturer's protocol with minor adjustments (the digestion step was performed for 1 hour).

After double digestion, both cut plasmid and PCR product were purified again before the ligation reaction.

Ligation reaction was performed as below:

Component	Amount
Linear pME vector	50 ng
PCR product	26 ng (1:3)
10X T4 DNA Ligase	2 µl
Nuclease-free water	To 20 ul

Ligation was performed for 1 hour at 22°C. Ligation product then directly transformed to bacteria.

2.2.2.6. Transformation of plasmids

Transformation of plasmids were performed according to their antibiotic resistance and presence of suicide gene *ccdb.* ccdb containing plasmids were pDONR and pDEST. All entry vectors are transformed to *JM109 E.coli* strain according to protocol. pME-asyn and final destination vectors were transformed to *DH5alpha* strain. Chemical transformation protocol was applied to all present plasmids as described below.

2 µl of plasmids were inoculated to 50 µl chemically competent bacteria on ice near the flame. After inoculation, it was waited for 30 min on ice. 30-sec heat shock at 42°C was performed to facilitate the entrance of plasmid to bacteria. Then, it was immediately

placed back on ice for 5 minutes. The mixture was placed in liquid prewarmed LB to initiate growth and placed in a shaker incubator at 37°C for 1 h. Lastly, 50 µl of this mix was inoculated to antibiotic resistance agar plates and incubated for 18 h at 37°C incubator. Plasmids were validated with colony PCR as well as NGS after miniprep amplification.

Table 2.8. Colony PCR primers used in this study

Name	**5' - 3' Sequence**	**Tm**	**Length**
Transposase_F	GCCTAGTGTCCATCAGTTAAG	52,6	21
Transposase_R	CTCGTATGTTGTGTGGAATTG	51,7	21
Mcher_F	TTCTGCTTAGTTTGATGCCTG	53,1	21
Mcher_R	TGGTCTTCTTCTGCATTACG	52,4	20
Ubi_F	TTTGTGATGCTCGTCAGG	52,5	18
Ubi_R	AGTAGTTGATTCATAGTGACTGG	51,8	23

2.2.2.7. Miniprep plasmid isolation protocol

To isolate and create stocks of each vector, miniprep plasmid isolation protocol was applied. For this purpose, NucleoSpin Minikit (Macherey Nagel) was used according to the manufacturer's protocol. Briefly, 1-5 ml of overnight culture E. coli culture was centrifuged to get cell pellet for 30 s at 11.000 x g. After discarding the supernatant, 250 µl of resuspension buffer (A1 buffer) was added, and the pellet was completely dissolved using vortex. 250 µl of lysis buffer (A2 buffer) was added and mixture was gently mixed by inverting 6-8 times. After 5 minutes of incubation at room temperature, neutralization buffer (A3) was added and mixed by inversion until the solution became colorless. When neutralization was completed, mixture was centrifuged for 5 min at 11.000 x g. The clear

supernatant was carefully transferred to the isolation column for binding of plasmid DNA. Columns were centrifuged for 1 min at 11.000 x g, and flow-through was discarded. Silica columns were washed with Buffer A4 and centrifuged again. Lastly, 50 µl of elution buffer column was added to the column. Plasmid DNAs were eluted to a sterile 1.5 ml microcentrifuge tube, and concentrations were measured by Nanodrop 2000.

2.2.2.8. Gateway recombination

The final recombination of all three vectors into a single expression vector was performed using LR recombination. LR Clonase enzyme was used to perform this reaction, and calculations were made using Mosimann's calculations based on equimolar ratios of plasmids [109].

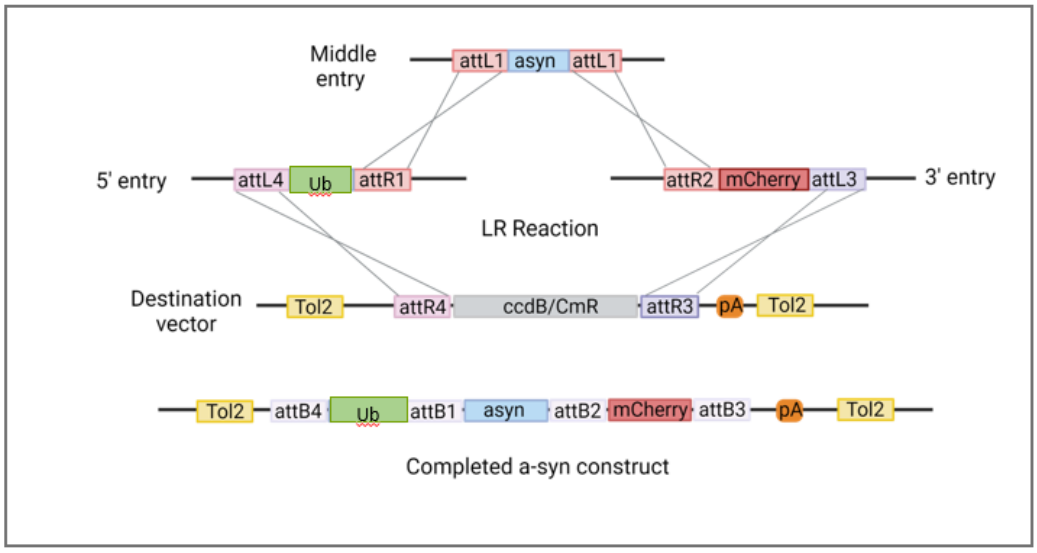

Figure 2.2. Final α-syn expression construct development using Multisite gateway cloning

Plasmid Name	bp total	fmol	Total	Plasmid Concentration (ng/µl)	Use (µl)
pUbi	6282	20	82,92 ng	40	1,03
pME-Asyn	3032	20	40,02 ng	40	0,5
P3E-mCherry	3550	20	46,86 ng	40	0,58
pDEST	7796	20	102 ng	40	1,28
Add 0,59µl nuclease-free water, then add 1 µl LR Clonase to get 5 µl reaction mix					

Two crucial points should be considered while setting up the recombination reaction. First, over-concentrated vector solutions should be avoided; 20-60 ng/µl is ideal. Second, LR Clonase should be thawed on ice before mixing, and it should be vortexed thoroughly. LR recombination was performed at 25°C overnight. The next day, the reaction was terminated using Proteinase K at 37°C for 15 min. The end product was transformed into bacteria and screened for positive clones via colony PCR and next-generation sequencing.

2.2.2.9. Next-generation sequencing

Following the establishment and confirmation of constructs via colony PCR, each colony carrying the appropriate plasmid was inoculated in the LB media. The isolated plasmids were subjected to quantification using a NanoDrop Spectrophotometer. Subsequently, 1000 ng of plasmid DNA was prepared for NGS analysis based on the plasmid DNA concentration. NGS results were obtained from the company-provided file in FASTA format, while the plasmid maps were acquired through the Benchling tool.

2.2.2.10. In vitro transcription of transposase

The transposase plasmid was transformed and isolated, similar to the other plasmids

stated above. After miniprep, the plasmid was linearized using NotI enzyme according to the manufacturer's protocol. The linearized plasmid was purified, and for each IVT reaction, 2 µg linearized plasmid was used.

Component	Amount
Linear Template	2 µg
2X NTP/CAP	10 µl
10X Reaction Buffer	2 µl
Enzyme Mix	2 µl
Nuclease-free water	To 20 µl

Reaction was incubated at 37°C for 2h. Purification was performed using LiCl precipitation and concentrations were measured using Nanodrop. Also, integrity of RNA was controlled by running on gel. Samples were aliquoted and stored at -80°C for further usage.

2.2.3. Zebrafish experiments

2.2.3.1. Zebrafish husbandry and maintenance

In this study, all fish were maintained in the Bilkent University Zebrafish Facility. The system keeps the water temperature at 28 °C and maintains the pH between 7.0 and 7.5. Animals were maintained in tanks with a 14-h light and 10-h dark cycle. Fish were fed twice daily with dry flakes and once fresh artemia. In this setup, we used young (3 months old) and old (2 years old) GFAP: GFP fish and AB WT fish for transgenic development. Ethics decision was dated 22/12/2021 (No:2021/18)

2.2.3.2. Breeding and Injections of Expression Vector

Breeding setups were prepared the day before to perform injections. Male and female AB wildtype fish were taken into the mating tank, fed, and kept with the separator. The separators opened the next day in the early morning, and the fish were waiting to lay eggs. The eggs obtained were collected and checked under a microscope to get fertilized eggs. Embryos should be injected at the 1 to 4-cell stage to provide a homogeneous vector expression.

To perform injections, 100 embryos were placed in an injection mold on a petri dish filled with E3 medium. The injection solution was prepared as 1 ul of 20ng/µl transposase mRNA, 4 ul of 80 ng/µl α-syn plasmid, and 1 µl tracking dye, completing to 10 ul with nuclease-free water on ice. The solution was loaded into a pulled glass capillary needle with micro loader pipette tips. The tip of the capillary needle was broken under a stereomicroscope, and each embryo was injected with 2 nl solution. The injection syringe pump was set to 100 µl /hr dispensation rate with 8 mm diameter (syringe diameter). Embryos were checked after injection, and dead ones were removed. Injected embryos were placed in fresh E3 medium and incubated at 28°C incubator. Embryos were monitored daily and checked for mCherry signal under a fluorescent microscope.

2.2.3.3. Genotyping

Two-week-old fish were anesthetized by immersion in 0.02% MS-222 (Tricaine) at neutral pH until their movement was slowed. Then, the anesthetized fish were transferred into a clean petri dish, and the tail fins were clipped. During this process, it should be important not to cause bleeding. The fish were then immediately transferred to a new plate with fresh system water individually and monitored until recovery. In optimal

conditions, fish should regain the ability to swim in 5 minutes.

For DNA isolation, each fin clip was placed into 1.5 ml sterile tubes, and then 100 µl DNA Lysis Buffer was added. The tubes were vortexed for 30 sec. Initial incubation was performed at 98°C for 10 min. Then, 2 µl of Proteinase K was added and incubated at 55°C overnight. Proteinase K was inactivated at 98°C for 10 min the next day. Centrifugation at 13000 rpm for 10 min was performed, and the supernatant was collected in a new 1.5 microcentrifuge tube.

For genotyping PCR, 1 µl of genomic DNA extract was used.

Component	**Amount**
Template DNA (200 ng/µl)	1 µl
Asyn Forward Primer (0.5mM) 5'CGACGACAGTGTGGTGTAAAG'3	1 µl
Asyn Reverse Primer (0.5 mM) 5'CTCAAGAAACTGGGAGCAAAG'3	1 µl
2X Taq polymerase with Red Dye	5 µl
Nuclease-free water	To 10 µl

PCR conditions were 95°C 5 min initial denaturation, 35 cycles of 95°C for 30 sec, 57°C for 40 sec, 72°C for 40 sec and final elongation at 72°C for 5 min.

PCR products were run on 1.5% agarose gel at 90V for 1h to visualize correct position of the bands.

2.2.3.4. Cerebroventricular microinjection (CVMI) and peritoneal injections of α-syn fibrils

To perform injections on three-month-old and two-year-old zebrafish, fish were gradually anesthetized with ice water. Then, anesthetized fish were stabilized using a wet sponge to facilitate correct orientation and avoid hypoxia in animals.

For cerebroventricular injections, fish were positioned as the head is located upside. The skull was punched with an insulin needle first, then using a Hamilton syringe and thin needle, a 10 µl injection solution was performed to the telencephalon region of the brain. For peritoneal injections, fish were positioned upside down. Intraperitoneal injections were performed directly with a Hamilton syringe into the abdominal cavity, posterior to the pelvic girdle.

After both injections, fish were immediately transferred to system water for recovery. Fish that were showing neurological abnormalities were euthanized and dissected.

2.2.3.5. Tissue preparation and cryosectioning

Euthanized fish were dissected for both brain and gut, and tissues were collected in sterile PBS solution on ice. Then, overnight fixation was performed using a 4% paraformaldehyde solution. After the fixation step, each tissue was washed three times for 5 min with PBS on a shaker with minimal rotation. Tissues were dehydrated in 10%, 20%, and 30% sucrose solution, respectively. Time was dependent on the sinking of the tissue in the sucrose solution. However, in each case, tissues were kept in 30% sucrose solution overnight. After cryoprotection, both gut and brain tissues were taken and embedded in O.C.T. product and directly stored in -80°C for sectioning next day.

Sectioning of the tissues was performed with Leica cryostat equipment. Tissues in O.C.T. were detached from the mold and stabilized in the cryostat's sample holder with O.C.T. The cryostat's temperature was fixed to -30°C. Sections were taken at 15 to 25 µm thickness, depending on the tissue integrity.

Sections were transferred carefully to HistoBond adhesive slides and dried quickly by heating them. Then, all slides were stored at -20°C until staining was performed.

2.2.3.6. Staining

For antibody stainings, slides were held at room temperature for an hour beforehand. They were washed three times, each for 5 minutes in 1X TBS-Triton X-100 solution at room temperature. After drying, tissue section borders were defined using a PAP pen. All slides were placed in petri dishes with wet paper towels to create a humid chamber and avoid evaporation of antibody solutions from sections. A blocking solution that contains 5%BSA in TBS-Triton X-100 was applied to each section to completely cover the sample and incubated at room temperature for 2 hours. After blocking, the solution was discarded carefully, and primary antibodies listed above were applied to sections and incubated at 4°C overnight. After primary incubation, slides were washed five times for 5 minutes with TBS-Triton X-100 and air-dried slightly. Secondary antibodies were applied onto sections, and 2 hours of incubation in a dark chamber was performed at room temperature. Lastly, all slides were washed with TBS solution, and DAPI staining was performed for 10 minutes. Slides were washed with TBS twice and air-dried under a dark chamber again. Coverslips were stabilized onto slides with nail polish, and images were taken with Leica SP8 Confocal Microscope with 20X, 40X, and 63X magnifications.

CHAPTER 3

3. RESULTS

3.1. Validation of amplified alpha-synuclein sequence

Firstly, amplified PCR bands were visualized on ChemiDoc equipment to validate α-syn gene products to ensure that the correct band sizes were present. Since it only gives information about the size, bands were isolated from the gel and resulting products were sent to Sanger Sequencing for validation. The resulting bands gave the correct size (423bp) as expected (Figure 3.1.), and sequencing also supported that successful amplification of human α-syn coding sequence was achieved (Figure 3.2.)

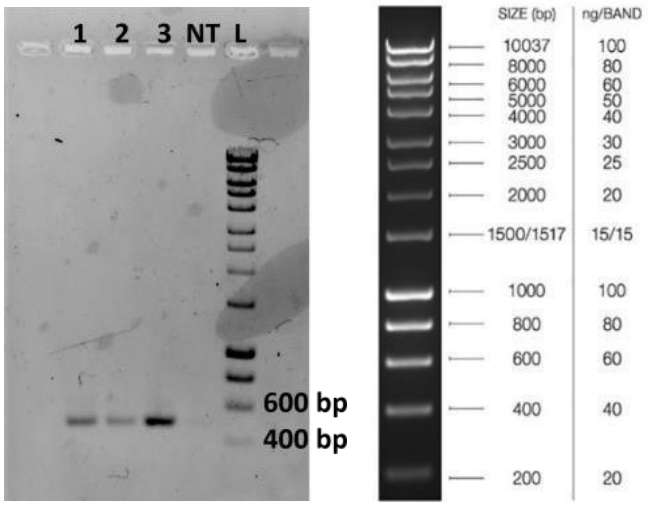

Figure 3.1.PCR products of α-syn visualized after agarose gel electrophoresis. **1-2-3:** products from different cDNA samples, **NT:** no template control. Bioline HyperLadder 1kb was used as a reference.

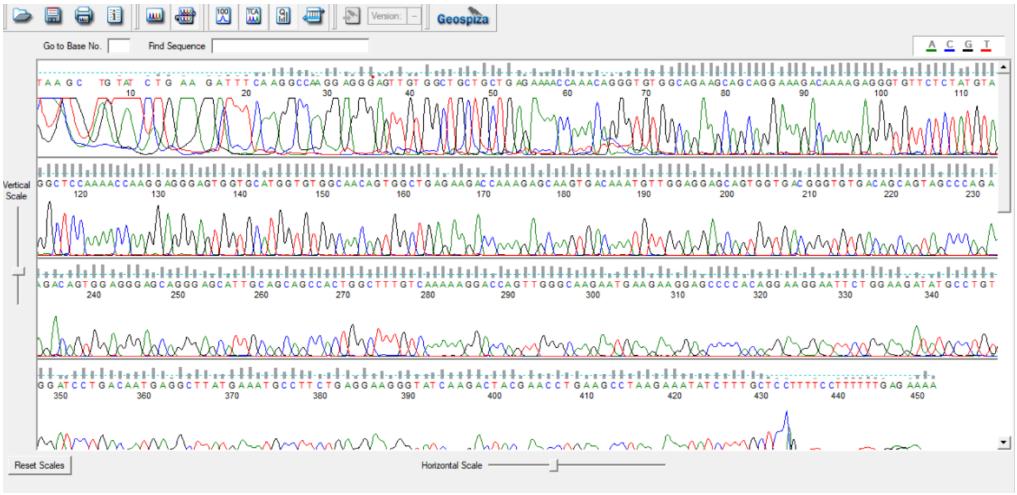

Homo sapiens synuclein alpha (SNCA), transcript variant 1, mRNA

Sequence ID: NM_000345.4 Length: 3177 Number of Matches: 1

Range 1: 248 to 664 GenBank Graphics ▼ Next Match ▲ Previous Match

Score	Expect	Identities	Gaps	Strand
745 bits(825)	0.0	416/417(99%)	1/417(0%)	Plus/Plus

```
Query  18   TTTCAA-GGCCAAGGAGGGAGTTGTGGCTGCTGCTGAGAAAACCAAACAGGGTGTGGCAG  76
            |||||| ||||||||||||||||||||||||||||||||||||||||||||||||||||
Sbjct  248  TTTCAAAGGCCAAGGAGGGAGTTGTGGCTGCTGCTGAGAAAACCAAACAGGGTGTGGCAG  307

Query  77   AAGCAGCAGGAAAGACAAAAGAGGGTGTTCTCTATGTAGGCTCCAAAACCAAGGAGGGAG  136
            ||||||||||||||||||||||||||||||||||||||||||||||||||||||||||||
Sbjct  308  AAGCAGCAGGAAAGACAAAAGAGGGTGTTCTCTATGTAGGCTCCAAAACCAAGGAGGGAG  367

Query  137  TGGTGCATGGTGTGGCAACAGTGGCTGAGAAGACCAAAGAGCAAGTGACAAATGTTGGAG  196
            ||||||||||||||||||||||||||||||||||||||||||||||||||||||||||||
Sbjct  368  TGGTGCATGGTGTGGCAACAGTGGCTGAGAAGACCAAAGAGCAAGTGACAAATGTTGGAG  427

Query  197  GAGCAGTGGTGACGGGTGTGACAGCAGTAGCCCAGAAGACAGTGGAGGGAGCAGGGAGCA  256
            ||||||||||||||||||||||||||||||||||||||||||||||||||||||||||||
Sbjct  428  GAGCAGTGGTGACGGGTGTGACAGCAGTAGCCCAGAAGACAGTGGAGGGAGCAGGGAGCA  487

Query  257  TTGCAGCAGCCACTGGCTTTGTCAAAAAGGACCAGTTGGGCAAGAATGAAGAAGGAGCCC  316
            ||||||||||||||||||||||||||||||||||||||||||||||||||||||||||||
Sbjct  488  TTGCAGCAGCCACTGGCTTTGTCAAAAAGGACCAGTTGGGCAAGAATGAAGAAGGAGCCC  547

Query  317  CACAGGAAGGAATTCTGGAAGATATGCCTGTGGATCCTGACAATGAGGCTTATGAAATGC  376
            ||||||||||||||||||||||||||||||||||||||||||||||||||||||||||||
Sbjct  548  CACAGGAAGGAATTCTGGAAGATATGCCTGTGGATCCTGACAATGAGGCTTATGAAATGC  607

Query  377  CTTCTGAGGAAGGGTATCAAGACTACGAACCTGAAGCCTAAGAAATATCTTTGCTCC  433
            |||||||||||||||||||||||||||||||||||||||||||||||||||||||||
Sbjct  608  CTTCTGAGGAAGGGTATCAAGACTACGAACCTGAAGCCTAAGAAATATCTTTGCTCC  664
```

Figure 3.2. Validation of purified PCR products with Sanger sequencing. Sequencing data was checked with FinchTV for read quality, then aligned with human α-syn coding sequence using BLASTn.

3.2. Cloning α-syn coding sequence to create middle entry clone

After the amplification of α-syn to create the middle entry clone for recombination, the addition of KpnI and SmaI cut sites was performed via a second round of PCR. Again, agarose gel electrophoresis was performed to observe the correct band size (Figure 3.3-

a). Also, the pME-MCS plasmid was cut with KpnI and SmaI enzymes to ligate the insert (Figure 3.3-b) further.

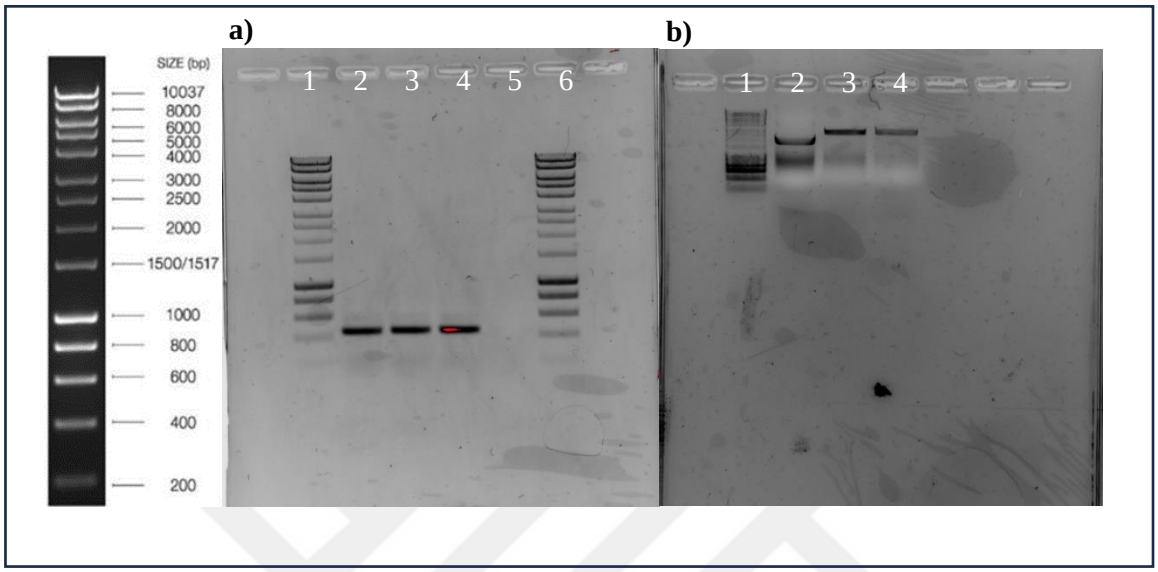

Figure 3.3. **a)** PCR products of α-syn after adding cut sites to each end. **b)** Double digestion (KpnI- SmaI) product of pME-MCS vector.

Ligation was performed after double digestion of the PCR product and the backbone vector with restriction enzymes. The ligation product was transformed into bacteria and characterized by restriction digestion after miniprep (Figure 3.4), along with a next-generation sequence analysis to validate the integration.

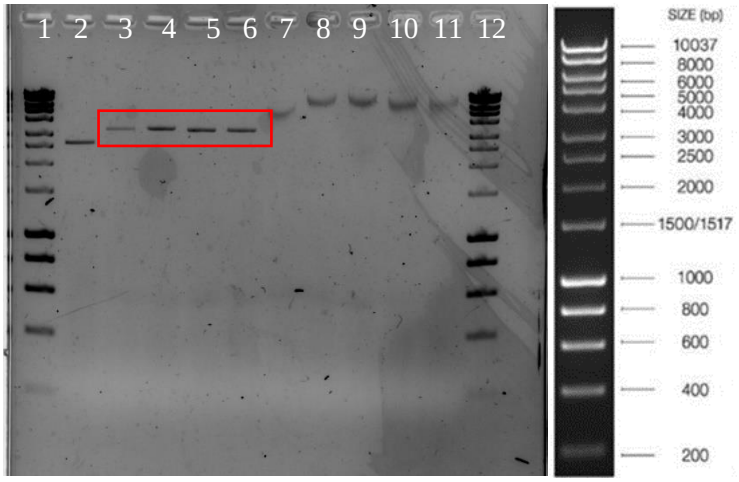

Figure 3.0.4. Validation of pME-asyn plasmid after miniprep with single restriction digestion with ApaI enzyme. Lanes 1,12: Ladder, Lane 2: backbone without ligation (2765 bp), Lane 3,4,5,6: correct clones (3032 bp), Lanes 7,8,9,10,11: wrong clones digestion with ApaI enzyme. Lanes 1,12: Ladder, Lane 2: backbone without ligation (2765 bp), Lane 3,4,5,6: correct clones (3032 bp), Lanes 7,8,9,10,11: wrong clones

The final version of the plasmid map was drawn using Benchling and represented in Figure 3.5.

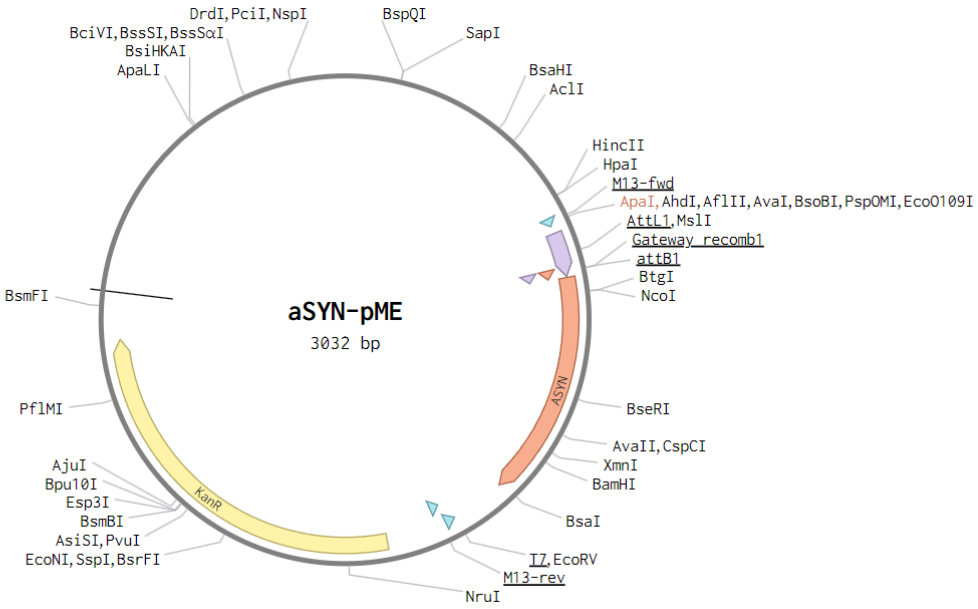

Figure 3.5..Representative map of pME-α-syn after sequencing

3.3. Validation of other plasmids

Validations of other plasmids were performed by either colony PCR after transformation or restriction enzyme digestion after miniprep of selected colonies. pCS2FA-transposase, pUbi, p3E-mCherry, and pDest vectors were sequenced and validated. Sequence information of entry vectors according to sequencing results is represented in Appendix Table 1. All plasmids' maps were drawn according to sequences using Benchling (Figure 3.6.).

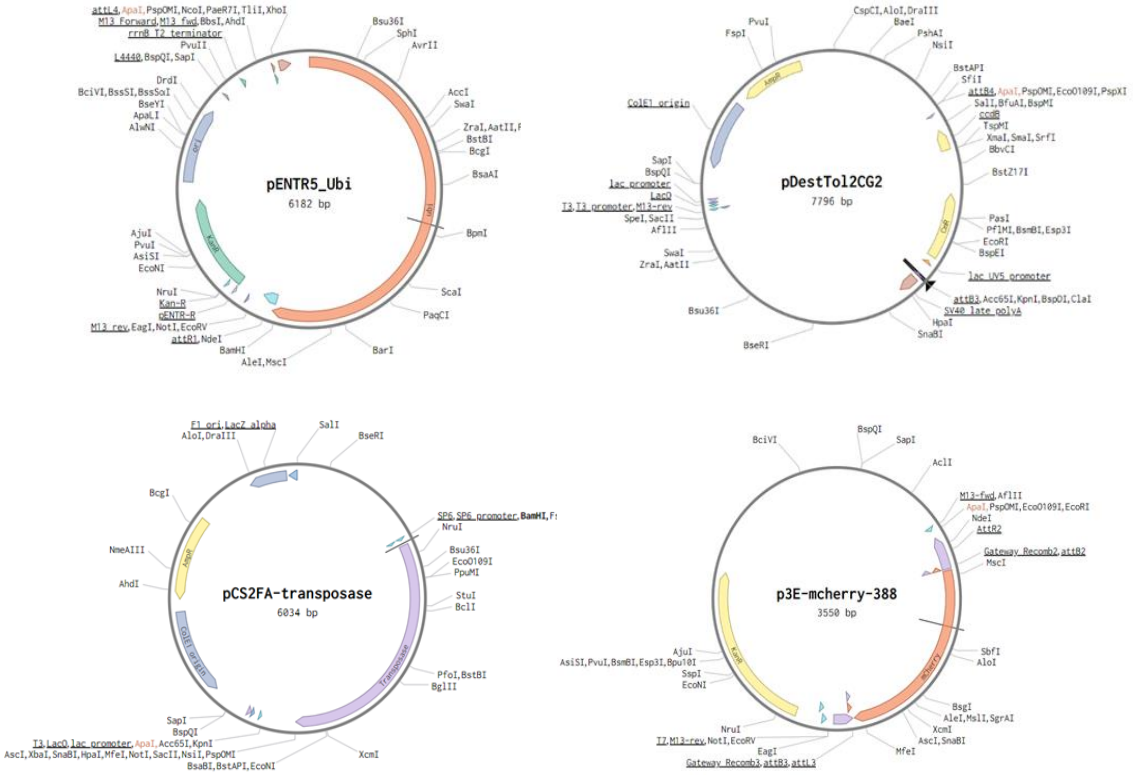

Figure 3.6. Representative plasmid maps of other plasmids according to sequencing data. Drawn in Benchling.

3.4. Final expression vector construction by gateway cloning and validation

Final expression vector construction was performed as described in the methods part. The expected size of the vector was around 11kb after recombination. As a result of LR recombinations, colonies were picked from agar plates, and colony PCR and PCR after minipreps were performed to validate that both α-syn and mCherry sequences were present. As expected, some colonies were false positives. Therefore, colonies showing both positive PCR products were chosen to be further amplified (Figure 3.7, Figure 3.8).

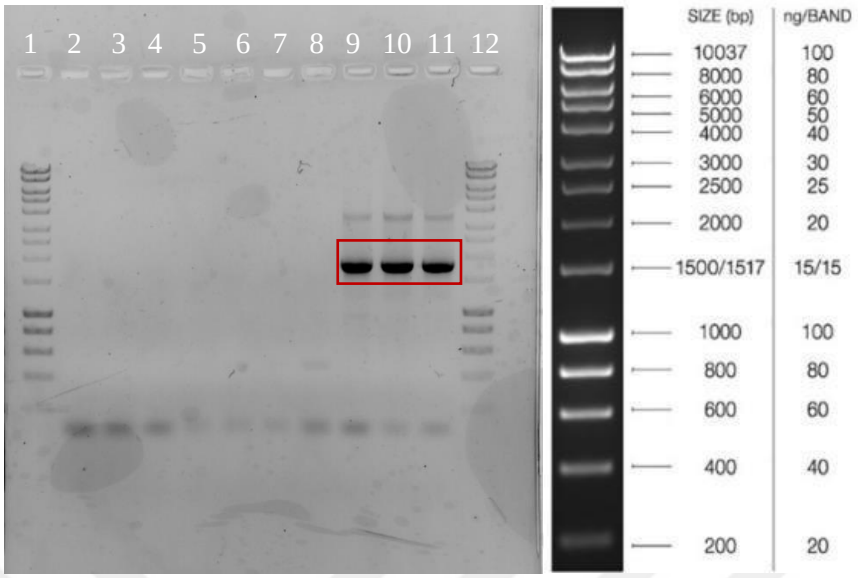

Figure 3.7.Validation mCherry sequence via colony PCR after LR recombination on agarose gel. The expected band size was 1690 bp. Three clones marked with red square are correct since they gave the right size.

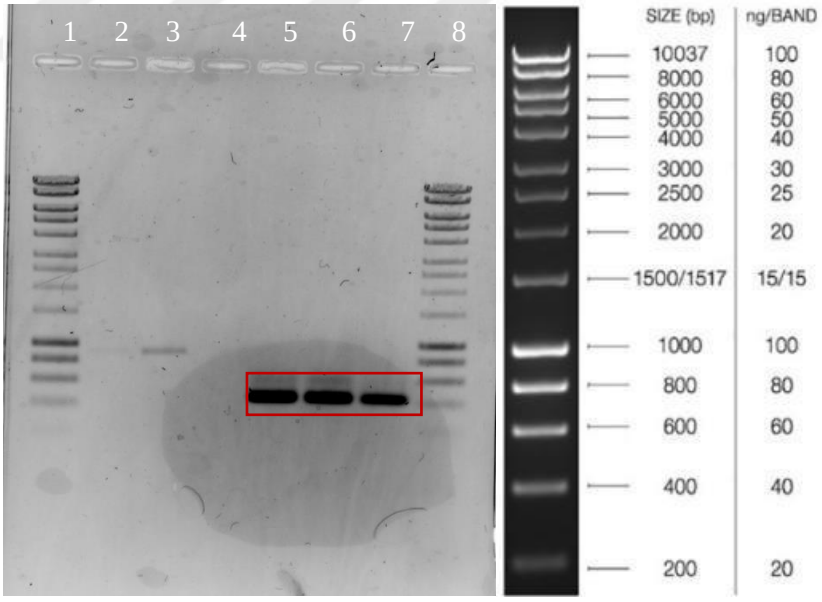

Figure 3.8. Validation of α-syn sequence via colony PCR after LR recombination on agarose gel. The expected band size was 423 bp. Three clones marked with red are positive, and these colonies gave both the right size mCherry and α-syn PCR products.

Positive clones detected by colony PCR were isolated by miniprep and sent for next-generation sequencing to detect the full map. The final expression plasmid containing all three entry vectors was defined by sequence, and the map was drawn on Benchling (Figure 3.9).

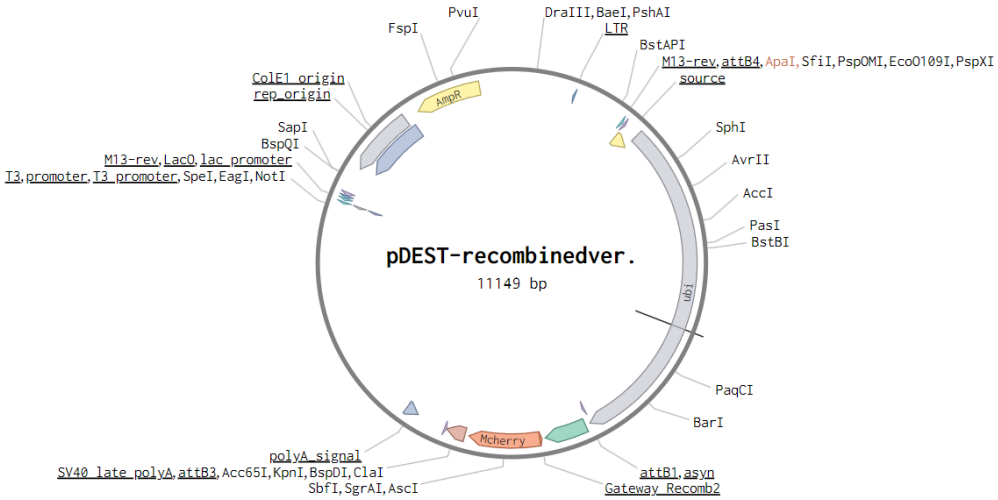

Figure 3.9. The final expression vector map was drawn according to the sequencing of the plasmid product using Benchling.

3.5. In vitro transcription of transposase mRNA and validation

Transposase mRNA is required for stable integration of target gene construct to genome. It could be co-injected as a plasmid with expression plasmid. However, the efficiency of the expression drastically changes in that condition. Therefore, presenting transposase mRNA directly secures faster integration of the genetic material into the zebrafish genome. By using mMessage mMachine Kit, transposase mRNA was synthesized from pCS2FA-transposase. The resulting mRNA concentration was detected as 1023 ng/µl by using a Nanodrop 2000 spectrophotometer. RNA integrity was also detected by running on agarose gel in the absence and presence of DNaseI (Figure 3.10).

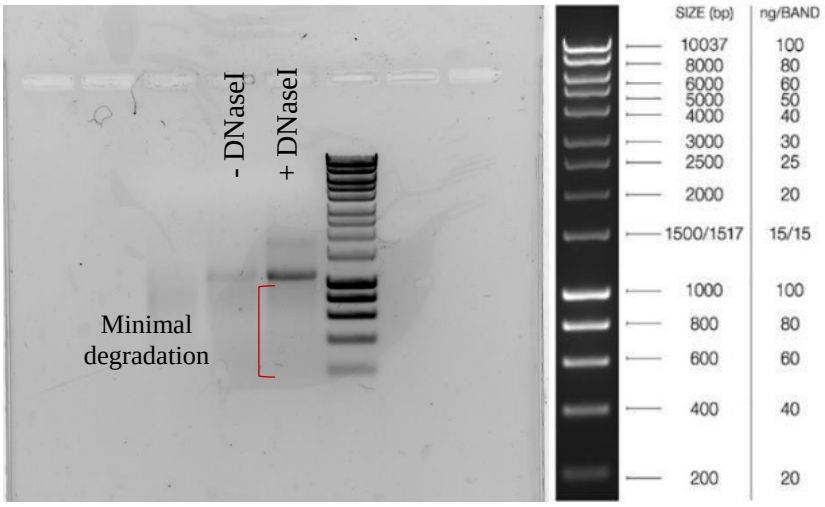

Figure 3.10. Transposase mRNA that was obtained after in vitro transcription. In the presence and absence of the DNase I enzyme, the integrity of the mRNA was observed. Target mRNA length was observed at the expected size of around 1000 bp. Hyperladder 1 kb DNA ladder was used as a reference.

3.6. Transgenic zebrafish development and genotyping

After the final expression vector was validated, transposase and destination vectors were co-injected into the one-cell stage of zebrafish. Zebrafish were checked for fluorescence signal at 4, 5, and 6 d.p.f. to observe the mCherry signal using fluorescence microscopy; however, the signal was inadequate.

To guarantee the integration of alpha-synuclein into the zebrafish genome, genotyping was performed on two-week-old zebrafish. DNAs isolated from tail samples of individual fish were amplified for α-syn presence, and PCR products were run on a gel to observe whether the band size was correct (Figure 3.11). Given that, the right product was observed on eleven fish on the same gel; others also contained a high number of positive α-syn integrations.

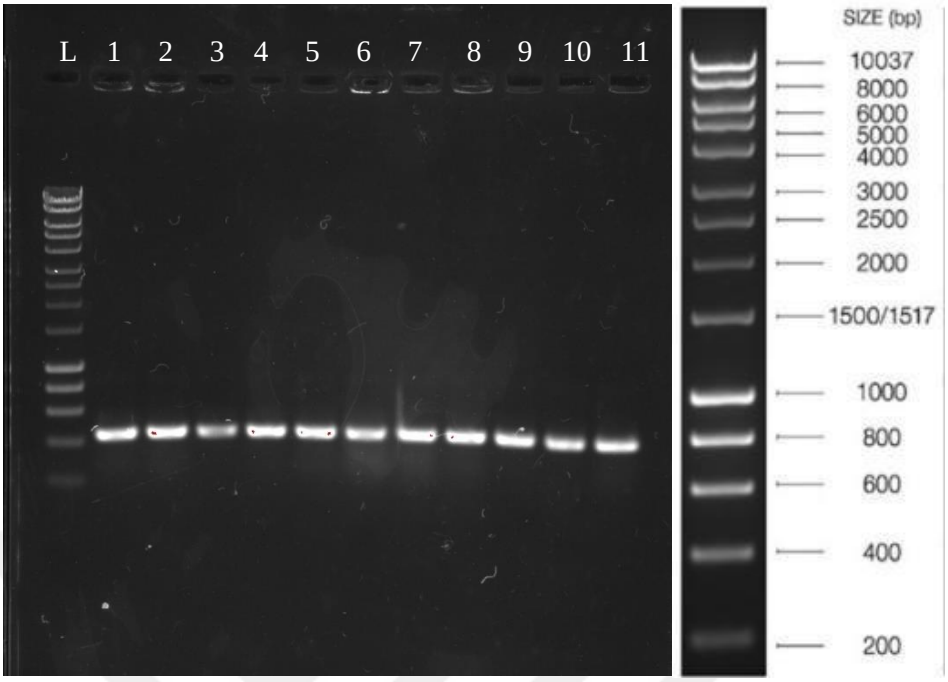

Figure 3.11. Genotyping of zebrafish for alpha-synuclein presence. PCR products (423bp) were loaded on agarose gel and ran for 40 min at 90V. Bioline HyperLadder 1kb was used.

3.7. Immunohistochemistry

Immunostainings were performed to observe alpha-synuclein fibril presence and how it aggregates and travels through the body of zebrafish in both young (3 months old) and old (2 years old) zebrafish. According to our observations, after 1-h post-injection, there was a high presence of fibrils in the brain, especially in the ventricular cavity between each hemisphere in the brain (Figure 3.12. & Figure 3.14-a). In old zebrafish, the presence of fibrils after one week persists in highly in the ventricular zone of telencephalon (TeV) (Figure 3.13) which is responsible for generating new precursor cells and neurons. Fibrils were co-stained with synaptophysin, a synaptic transmission marker for neurons, and co-localization was observed in that area (Figure 3.13).

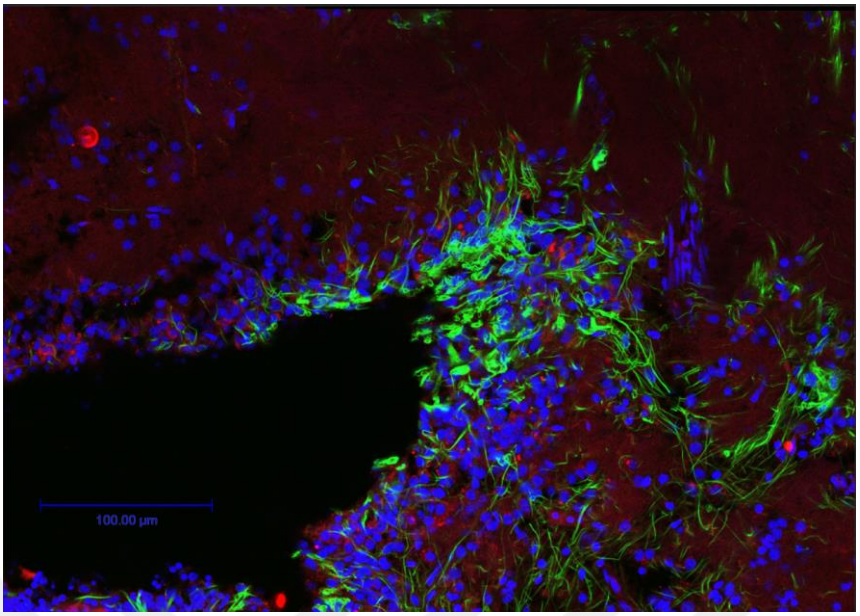

Figure 3.12. α-syn fibril presence in old zebrafish (2yo) after 1-h post-CVMI injection. Green: α-syn, Blue: DAPI, red: synaptophysin. Scale bar: 100µm

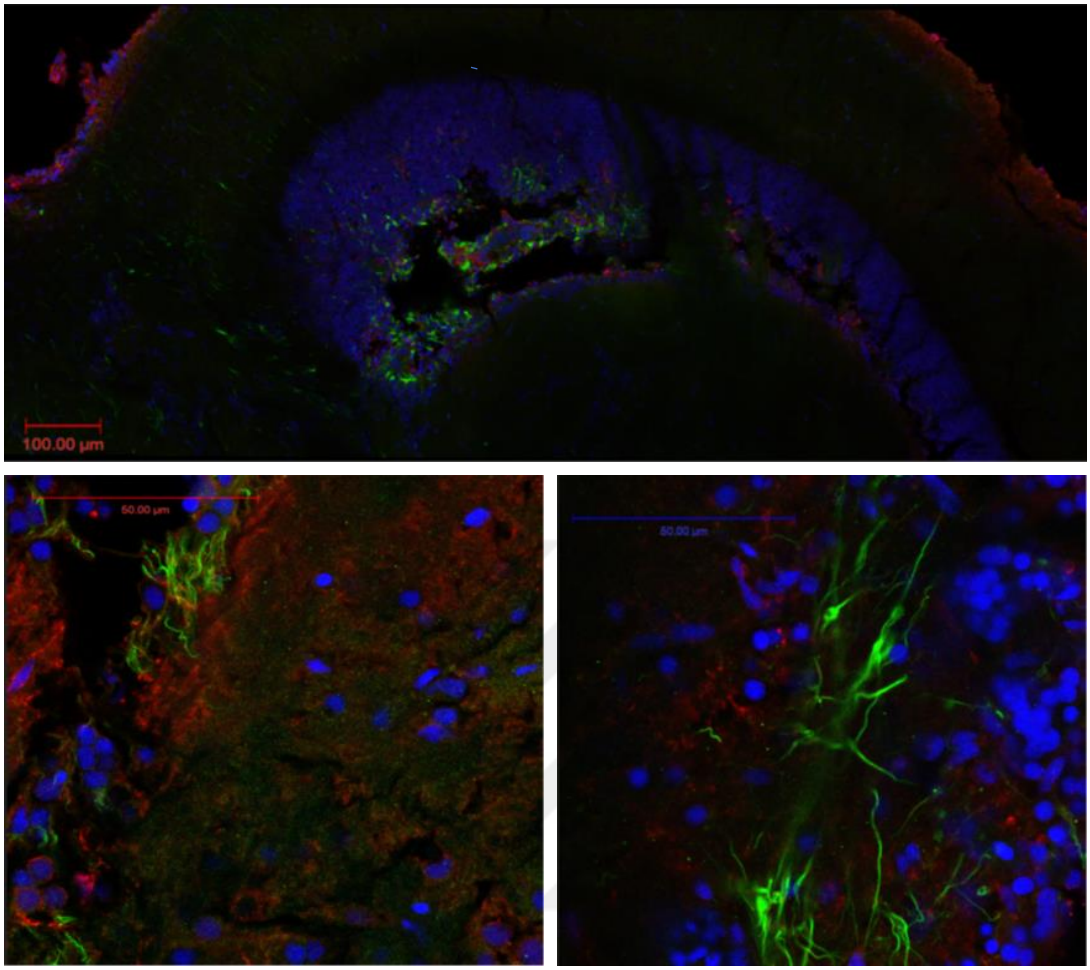

Figure 3.13. α-syn fibril presence in old zebrafish (2yo) after one-week post-CVMI injection. Green: α-syn, Blue: DAPI, red: beta-tubulin. Scale bar: 100µm

Even though fibrils were observed in the brains of young zebrafish after CVMI, their density was lower than that of old zebrafish. After one week of injection, fibril density was even lower compared to old zebrafish possibly due to the regeneration power of the young zebrafish (Figure 3.14).

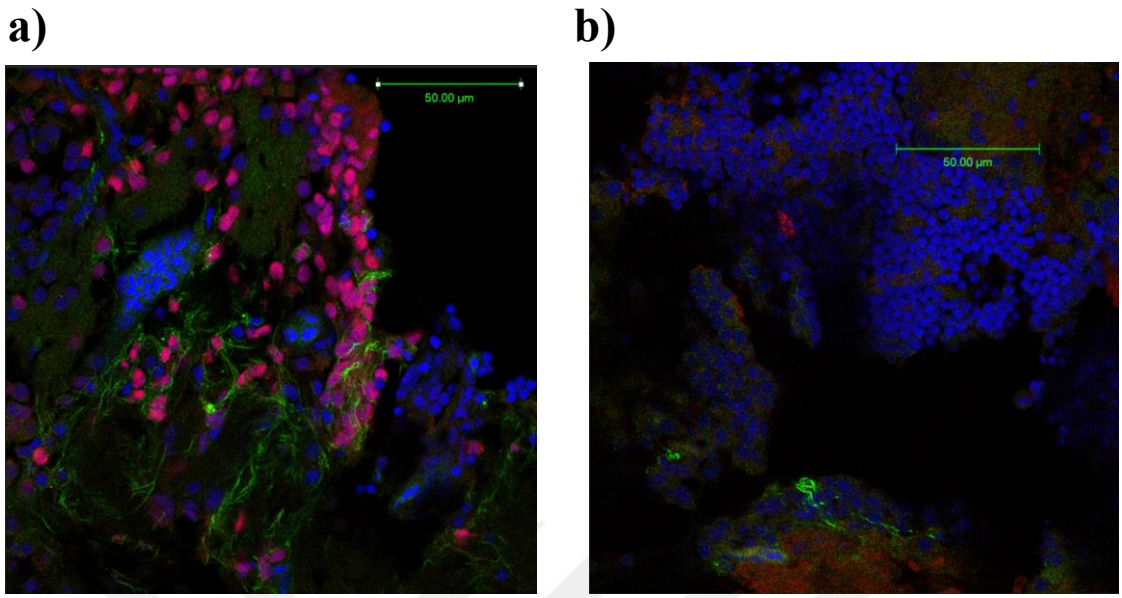

Figure 3.14. α-syn fibril presence in young (3 mo) zebrafish after a) 1h post-injection and b) 1-week post-injection to the brain. Blue: DAPI, Green: α-syn, red: beta-actin. Scale bar: 50 µm

Immunostainings were performed for alpha-synuclein in the gut to observe α-synuclein transmission between the brain and gut. Alpha-synuclein fibril presence was detected in gut epithelia after one week of CVMI injections of old zebrafish. This showed that even though the fibril form of α-syn is disrupted, it could travel to the gut and remain in the epithelia (Figure 3.15).

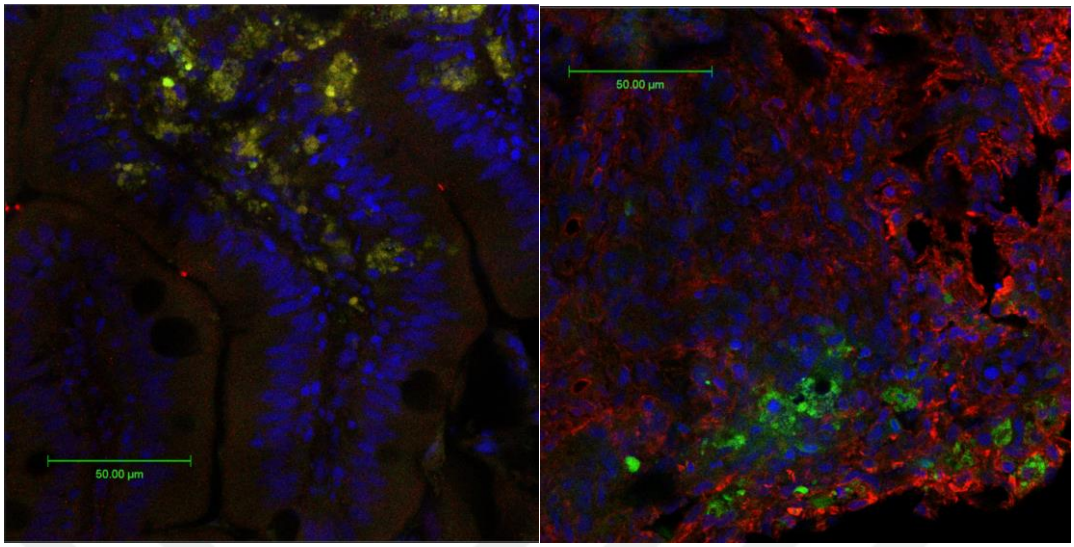

Figure 3.15. α-syn fibril presence in gut of old (2 yo) zebrafish after 1-week post-injection to the brain. Blue: DAPI, Green: α-syn, red: beta-actin. Scale bar: 50 µm

Travel from the brain to the gut could not be detected in young zebrafish, so it is not represented in the results. This could be due to the high regeneration power of young zebrafish, which could completely discard the fibrils and prevent their travel through the body. The aggregation of fibrils from the gut to the brain was also considered. While the observation of high numbers of α-syn in the gut epithelia is still present in young zebrafish after one-week post-injection peritoneally, fibrillization was highly disrupted. Also, we could not observe clear α-syn fibril staining in the fish brain in that condition (Figure 3.16).

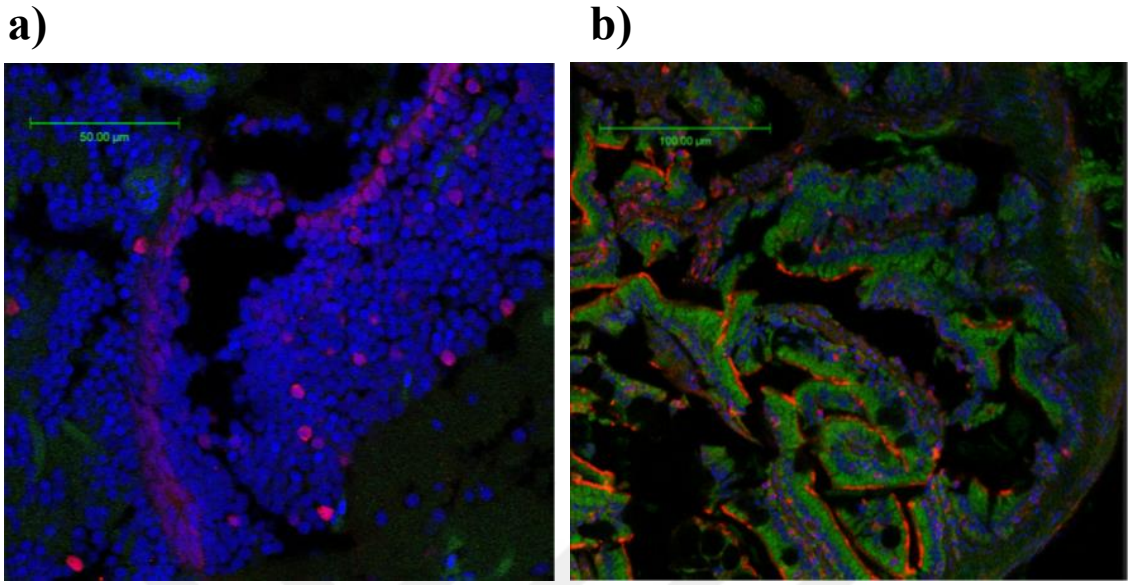

Figure 3.16. α-syn fibril presence in a) brain and b) gut of young (3 mo) zebrafish after 1-week post-injection intraperitoneally. Blue: DAPI, Green: α-syn, red: beta-actin. Scale bar: 50 µm, 100 µm respectively.

Further stainings and additional markers, such as dopaminergic neuron markers like TH and neuronal markers like beta-III tubulin, were needed to understand alpha-synuclein behavior better. Also, a larger cohort of animals could provide a better understanding of the results' consistency. However, even though fish do not express alpha-synuclein itself, human synuclein fibrils are still able to travel at some level from the brain to the gut, especially in aged fish.

CHAPTER 4

4. DISCUSSION

This thesis study primarily focuses on alpha-synuclein-dependent Parkinson's disease, modeling alpha-synuclein expressing transgenic zebrafish model and comparative effects of brain-first and body-first PD differences.

Parkinson's Disease is defined as the second most prevalent neurodegenerative disease, and it mainly affects aged populations. With the current aging trends in the world, number of people suffering from PD is expected to exceed 10 million in 20 years [110]. The first known drug is Levodopa, a precursor of dopamine that helps to restore dopamine levels. However, Levodopa administration is limited because of adverse effects [111]. Alternatives such as rasagiline, safinamide, and monoamine oxidase inhibitors are also potential drugs that increase the levels of dopamine. However, decreases in dopamine levels are only a consequence of disease in a small subset of PD patients, and it can be detected only in the clinical phase. To overcome all clinical symptoms, patients have to use a combination of many drugs, including serotonin regulators for depression, sleep regulators such as melatonin, and anticholinergic drugs for other motor symptoms [112]. Unfortunately, not all symptoms may be relieved, and patients suffer from the disease for an extended period of time.

New therapies mainly focus on reducing alpha-synuclein (α-syn) since abnormally

accumulating α-syn products are the leading cause of Lewy-body formation. α-syn is essential in regulating the dopamine pathway, mainly through regulating dopamine vesicle size and localization of the receptors on the membrane [113]. Its expression is highly present in brain regions such as substantia nigra, hippocampus, cerebellum, cortex, and hypothalamus, but not limited to the brain. Expression is also present in spinal cord, bone marrow, colon, heart, endometrium, ovary, and skin [114].

Recently, the initiation site of pathological alpha-synuclein and its accumulation route have become popular hypotheses for differentiating pathologies between patients. Investigation of how brain- and body-first subtypes differ in their initiation mechanisms and progression patterns was initially shown in PET scans and MRI data from patients [51]. However, the initial progression remains elucidated and needs to be focused on more. For this purpose, the generation of new animal models is necessary.

We aimed to develop a new transgenic model of human α-syn expressing zebrafish. Since zebrafish do not contain a gene homologous to the human version, forced expression of α-syn is mandatory to compare fibril progression in later studies [105]. In literature, some forms of the transgenic α-syn expressing zebrafish had limited lifespan. Therefore, while starting, it was also unknown to us if the animals would live. In a recent model by Lopez et al. [107], they developed both human wild-type and the most common mutant form (A53T) of α-syn in zebrafish. The wildtype model did not show any abnormalities in terms of lifespan. However, mutant model had a shorter life. This model only discussed the human α-syn expression on zebrafish and possible phenotypes as the most recent model in the literature. They only constructed expression of neuronal cells; therefore, using this or any other published model was unsuitable for us to study brain-first and gut-first PD. Hence, we developed a construct under a ubiquitous promoter that drives

constitutive expression in all tissues [115]. The construct was developed using an extensively method called multisite gateway cloning. Three component of the expression vector (promoter, target gene, and reporter gene) was recombined in a single backbone vector. Recombination was facilitated by using LR clonase enzyme mix which contains Integrase and Excisionase, which are bacteriophage lambda recombination proteins, and protein integration host factors [116]. This enzyme allows constructs to be prepared in vitro. After construction, zebrafish were injected with target construct and transposase mRNA to facilitate stable expression in zebrafish embryos. By using traditional PCR, transgenesis was validated for α-syn integrated zebrafish. Typically, we planned to observe mCherry signal in early larval stages (2 d.p.f to 6 d.p.f). However, we could not observe an adequate signal of mCherry. This might be due to the random introduction of an early stop codon before the mCherry coding sequence during recombination reactions. According to sequencing data, we did not observe any stop codon in ORF. However, single-point mutations may affect the expression capability of mCherry in vivo. In any case, imaging of fluorescence reporter needs to be performed with larger animal cohorts to ensure expression.

To observe the effects of preformed fibril injections, brain (CVMI) and body (peritoneal) injections were performed to confirm two modes of PD. As expected, we observed migration of α-syn between brain and gut and their localization. In aged zebrafish, migration was more detectable compared to young animals. This could be due to the regeneration potential of young zebrafish since zebrafish can regenerate many tissues, including heart, fin, and nervous system components [117]. When young zebrafish were injected peritoneally, although we could observe high densities of alpha-synuclein in gut after one week, there was no presence in the brain. This might be related to the

regeneration power of young zebrafish brains. Another point is that we found localized signals in the brain, especially in the region of the ventricular zone of the telencephalon, for CVMI injections. This might be due to the closeness of the injection area. However, it might be related that this region is highly proliferative, and branched axons mostly innervate in the telencephalon region. In the brain-first hypothesis, one of the primary emergence regions is also the telencephalon. In contrast, body-first PD shows late fibril accumulation in the telencephalon [118].

Overall, we tried to observe how initial transmission occurs between the brain and gut and how it relates to the organism's age. We developed a transgenic model to further test these two hypotheses, including other organs such as the heart, skin, and gonads.

CHAPTER 5

5. Conclusion and Future Perspectives

This study aimed to develop a new model to investigate Parkinson's disease, specifically two disease modes: brain-first and body-first PD. As discussed above, there are many models to study PD on zebrafish, either by chemical or genetic manipulations. However, these models still do not fully reflect how the disease progresses, and the effects of the emergence point in the body remain unclear.

Within this study's scope, we aimed to develop a new Parkinson's disease to study the brain-first and body-first hypotheses of PD using zebrafish. The generated model showed successful integration of α-syn into the zebrafish genome, with no adverse effects for up to 3 months. Expression levels of α-syn will be further confirmed by quantitative real-time PCR at the RNA level and Western Blot at the protein level. In addition, We observed alpha-synuclein transmission between the brain and the gut in zebrafish. We need to understand further the pathological differences in PFF-induced pathology between brain- and body-first PD. To check the injected fibrils diffusion among other tissues, neutral fluorescent dye injections will also be performed to detect diffusion rate throughout the body. The severity of infections and survival rate is another point that will be considered in the following studies. For this purpose, lifespan assays will be

performed after injections. Additional markers for immunohistochemistry to check mitochondrial stress, phosphorylation of alpha-synuclein, and synaptic integration will be added to assess the toxicity. Moreover, organs like heart and gonads will be also considered for alpha-synuclein accumulation in immunohistochemical analysis. Since PD is also associated with behavioral and cognitive changes, behavioral and memory function assays should be performed after the following months of injection. The next step for this study will be to inject preformed fibrils in transgenic models to compare severity and pathology progression for brain-first and body-first emergence of α-syn accumulation. In this way, we plan to confirm differences between the two modes of PD on molecular and behavioral levels, which will be tested for the first time on zebrafish.

Bibliography

[1] "Parkinson's Disease: Causes, Symptoms, and Treatments," National Institute on Aging. Accessed: Aug. 05, 2024. [Online]. Available: https://www.nia.nih.gov/health/parkinsons-disease/parkinsons-disease-causes-symptoms-and-treatments

[2] D. Twelves, K. S. M. Perkins, and C. Counsell, "Systematic review of incidence studies of Parkinson's disease," *Mov. Disord.*, vol. 18, no. 1, pp. 19–31, 2003, doi: 10.1002/mds.10305.

[3] A. Kouli, K. M. Torsney, and W.-L. Kuan, "Parkinson's Disease: Etiology, Neuropathology, and Pathogenesis," in *Parkinson's Disease: Pathogenesis and Clinical Aspects*, T. B. Stoker and J. C. Greenland, Eds., Brisbane (AU): Codon Publications, 2018. Accessed: Aug. 05, 2024. [Online]. Available: http://www.ncbi.nlm.nih.gov/books/NBK536722/

[4] L. Hirsch, N. Jette, A. Frolkis, T. Steeves, and T. Pringsheim, "The Incidence of Parkinson's Disease: A Systematic Review and Meta-Analysis," *Neuroepidemiology*, vol. 46, no. 4, pp. 292–300, 2016, doi: 10.1159/000445751.

[5] Y. H. Lee *et al.*, "Beneficial effect of estrogen on nigrostriatal dopaminergic neurons in drug-naïve postmenopausal Parkinson's disease," *Sci. Rep.*, vol. 9, no. 1, p. 10531, Jul. 2019, doi: 10.1038/s41598-019-47026-6.

[6] R. D. S. Prediger, "Effects of caffeine in Parkinson's disease: from neuroprotection to the management of motor and non-motor symptoms," *J. Alzheimers Dis. JAD*, vol. 20 Suppl 1, pp. S205-220, 2010, doi: 10.3233/JAD-2010-091459.

[7] K. Wirdefeldt, M. Gatz, Y. Pawitan, and N. L. Pedersen, "Risk and protective factors for Parkinson's disease: a study in Swedish twins," *Ann. Neurol.*, vol. 57, no. 1, pp. 27–33, Jan. 2005, doi: 10.1002/ana.20307.

[8] C. Váradi, "Clinical Features of Parkinson's Disease: The Evolution of Critical Symptoms," *Biology*, vol. 9, no. 5, p. 103, May 2020, doi: 10.3390/biology9050103.

[9] W. Poewe *et al.*, "Parkinson disease," *Nat. Rev. Dis. Primer*, vol. 3, no. 1, Art. no. 1, Mar. 2017, doi: 10.1038/nrdp.2017.13.

[10] M. Amboni, P. Barone, and J. M. Hausdorff, "Cognitive contributions to gait and falls: evidence and implications," *Mov. Disord. Off. J. Mov. Disord. Soc.*, vol. 28, no. 11, pp. 1520–1533, Sep. 2013, doi: 10.1002/mds.25674.

[11] R. Krüger *et al.*, "Classification of advanced stages of Parkinson's disease: translation into stratified treatments," *J. Neural Transm.*, vol. 124, no. 8, pp. 1015–1027, 2017, doi: 10.1007/s00702-017-1707-x.

[12] C. Marras and K. R. Chaudhuri, "Nonmotor features of Parkinson's disease subtypes," *Mov. Disord. Off. J. Mov. Disord. Soc.*, vol. 31, no. 8, pp. 1095–1102, Aug. 2016, doi: 10.1002/mds.26510.

[13] H. Braak, K. Del Tredici, U. Rüb, R. A. I. de Vos, E. N. H. Jansen Steur, and E. Braak, “Staging of brain pathology related to sporadic Parkinson’s disease,” *Neurobiol. Aging*, vol. 24, no. 2, pp. 197–211, 2003, doi: 10.1016/s0197-4580(02)00065-9.
[14] T. G. Beach *et al.*, “Unified staging system for Lewy body disorders: correlation with nigrostriatal degeneration, cognitive impairment and motor dysfunction,” *Acta Neuropathol. (Berl.)*, vol. 117, no. 6, pp. 613–634, Jun. 2009, doi: 10.1007/s00401-009-0538-8.
[15] C. Blauwendraat, M. A. Nalls, and A. B. Singleton, “The genetic architecture of Parkinson’s disease,” *Lancet Neurol.*, vol. 19, no. 2, pp. 170–178, Feb. 2020, doi: 10.1016/S1474-4422(19)30287-X.
[16] Y. Ben-Shlomo, S. Darweesh, J. Llibre-Guerra, C. Marras, M. S. Luciano, and C. Tanner, “The epidemiology of Parkinson’s disease,” *The Lancet*, vol. 403, no. 10423, pp. 283–292, Jan. 2024, doi: 10.1016/S0140-6736(23)01419-8.
[17] K. Kalinderi, S. Bostantjopoulou, and L. Fidani, “The genetic background of Parkinson’s disease: current progress and future prospects,” *Acta Neurol. Scand.*, vol. 134, no. 5, pp. 314–326, 2016, doi: 10.1111/ane.12563.
[18] S. Lesage and A. Brice, “Parkinson’s disease: from monogenic forms to genetic susceptibility factors,” *Hum. Mol. Genet.*, vol. 18, no. R1, pp. R48-59, Apr. 2009, doi: 10.1093/hmg/ddp012.
[19] M. Funayama, K. Nishioka, Y. Li, and N. Hattori, “Molecular genetics of Parkinson’s disease: Contributions and global trends,” *J. Hum. Genet.*, vol. 68, no. 3, pp. 125–130, Mar. 2023, doi: 10.1038/s10038-022-01058-5.
[20] M. H. Polymeropoulos *et al.*, “Mutation in the alpha-synuclein gene identified in families with Parkinson’s disease,” *Science*, vol. 276, no. 5321, pp. 2045–2047, Jun. 1997, doi: 10.1126/science.276.5321.2045.
[21] I. F. Mata, W. J. Wedemeyer, M. J. Farrer, J. P. Taylor, and K. A. Gallo, “LRRK2 in Parkinson’s disease: protein domains and functional insights,” *Trends Neurosci.*, vol. 29, no. 5, pp. 286–293, May 2006, doi: 10.1016/j.tins.2006.03.006.
[22] A. Brice, “Genetics of Parkinson’s disease: LRRK2 on the rise,” *Brain J. Neurol.*, vol. 128, no. Pt 12, pp. 2760–2762, Dec. 2005, doi: 10.1093/brain/awh676.
[23] Y. Xiong, T. M. Dawson, and V. L. Dawson, “Models of LRRK2 associated Parkinson’s disease,” *Adv. Neurobiol.*, vol. 14, pp. 163–191, 2017, doi: 10.1007/978-3-319-49969-7_9.
[24] “Autosomal dominant dopa-responsive parkinsonism in a multigenerational Swiss family - PubMed.” Accessed: Aug. 17, 2024. [Online]. Available: https://pubmed.ncbi.nlm.nih.gov/18342564/
[25] E. T. Williams, X. Chen, and D. J. Moore, “VPS35, the Retromer Complex and Parkinson’s Disease,” *J. Park. Dis.*, vol. 7, no. 2, pp. 219–233, 2017, doi: 10.3233/JPD-161020.
[26] E. Miura *et al.*, “VPS35 dysfunction impairs lysosomal degradation of α-synuclein and exacerbates neurotoxicity in a Drosophila model of Parkinson’s disease,” *Neurobiol. Dis.*, vol. 71, pp. 1–13, Nov. 2014, doi: 10.1016/j.nbd.2014.07.014.
[27] “Mutations in the parkin gene cause autosomal recessive juvenile parkinsonism - PubMed.” Accessed: Aug. 17, 2024. [Online]. Available: https://pubmed.ncbi.nlm.nih.gov/9560156/
[28] T. M. Dawson and V. L. Dawson, “The Role of Parkin in Familial and Sporadic Parkinson’s Disease,” *Mov. Disord. Off. J. Mov. Disord. Soc.*, vol. 25, no. 0 1, pp.

S32–S39, 2010, doi: 10.1002/mds.22798.
[29] M. Vizziello, L. Borellini, G. Franco, and G. Ardolino, “Disruption of Mitochondrial Homeostasis: The Role of PINK1 in Parkinson’s Disease,” *Cells*, vol. 10, no. 11, Art. no. 11, Nov. 2021, doi: 10.3390/cells10113022.
[30] H. Ariga, “Common mechanisms of onset of cancer and neurodegenerative diseases,” *Biol. Pharm. Bull.*, vol. 38, no. 6, pp. 795–808, 2015, doi: 10.1248/bpb.b15-00125.
[31] S. E. Oh and M. M. Mouradian, “Regulation of Signal Transduction by DJ-1,” *Adv. Exp. Med. Biol.*, vol. 1037, pp. 97–131, 2017, doi: 10.1007/978-981-10-6583-5_8.
[32] J. Burré, M. Sharma, and T. C. Südhof, “Cell Biology and Pathophysiology of α-Synuclein,” *Cold Spring Harb. Perspect. Med.*, vol. 8, no. 3, p. a024091, Mar. 2018, doi: 10.1101/cshperspect.a024091.
[33] T. Bartels, J. G. Choi, and D. J. Selkoe, “α-Synuclein occurs physiologically as a helically folded tetramer that resists aggregation,” *Nature*, vol. 477, no. 7362, pp. 107–110, Aug. 2011, doi: 10.1038/nature10324.
[34] P. Calabresi, A. Mechelli, G. Natale, L. Volpicelli-Daley, G. Di Lazzaro, and V. Ghiglieri, “Alpha-synuclein in Parkinson’s disease and other synucleinopathies: from overt neurodegeneration back to early synaptic dysfunction,” *Cell Death Dis.*, vol. 14, no. 3, pp. 1–16, Mar. 2023, doi: 10.1038/s41419-023-05672-9.
[35] G. Fusco *et al.*, “Direct observation of the three regions in α-synuclein that determine its membrane-bound behaviour,” *Nat. Commun.*, vol. 5, no. 1, p. 3827, May 2014, doi: 10.1038/ncomms4827.
[36] D. Sulzer and R. H. Edwards, “The physiological role of α-synuclein and its relationship to Parkinson’s Disease,” *J. Neurochem.*, vol. 150, no. 5, pp. 475–486, 2019, doi: 10.1111/jnc.14810.
[37] F. Favretto *et al.*, “The Molecular Basis of the Interaction of Cyclophilin A with α-Synuclein,” *Angew. Chem. Int. Ed.*, vol. 59, no. 14, pp. 5643–5646, 2020, doi: 10.1002/anie.201914878.
[38] A. Sidhu, I. Segers-Nolten, and V. Subramaniam, “Conformational Compatibility Is Essential for Heterologous Aggregation of α-Synuclein,” *ACS Chem. Neurosci.*, vol. 7, no. 6, pp. 719–727, Jun. 2016, doi: 10.1021/acschemneuro.5b00322.
[39] J. T. Bendor, T. P. Logan, and R. H. Edwards, “The function of α-synuclein,” *Neuron*, vol. 79, no. 6, pp. 1044–1066, Sep. 2013, doi: 10.1016/j.neuron.2013.09.004.
[40] M. Robotta, J. Cattani, J. C. Martins, V. Subramaniam, and M. Drescher, “Alpha-Synuclein Disease Mutations Are Structurally Defective and Locally Affect Membrane Binding,” *J. Am. Chem. Soc.*, vol. 139, no. 12, pp. 4254–4257, Mar. 2017, doi: 10.1021/jacs.6b05335.
[41] H. K. Chung, H.-A. Ho, D. Pérez-Acuña, and S.-J. Lee, “Modeling α-Synuclein Propagation with Preformed Fibril Injections,” *J. Mov. Disord.*, vol. 12, no. 3, pp. 139–151, Sep. 2019, doi: 10.14802/jmd.19046.
[42] C. R. Fields, N. Bengoa-Vergniory, and R. Wade-Martins, “Targeting Alpha-Synuclein as a Therapy for Parkinson’s Disease,” *Front. Mol. Neurosci.*, vol. 12, Dec. 2019, doi: 10.3389/fnmol.2019.00299.
[43] D. J. Surmeier, J. A. Obeso, and G. M. Halliday, “Selective neuronal vulnerability in Parkinson disease,” *Nat. Rev. Neurosci.*, vol. 18, no. 2, pp. 101–113, Feb. 2017, doi: 10.1038/nrn.2016.178.
[44] S. A. Ferreira and M. Romero-Ramos, “Microglia Response During Parkinson’s Disease: Alpha-Synuclein Intervention,” *Front. Cell. Neurosci.*, vol. 12, Aug. 2018, doi: 10.3389/fncel.2018.00247.

[45] L. Parnetti *et al.*, “CSF and blood biomarkers for Parkinson’s disease,” *Lancet Neurol.*, vol. 18, no. 6, pp. 573–586, Jun. 2019, doi: 10.1016/S1474-4422(19)30024-9.
[46] P. Calabresi, B. Picconi, A. Tozzi, and M. D. Filippo, “Dopamine-mediated regulation of corticostriatal synaptic plasticity,” *Trends Neurosci.*, vol. 30, no. 5, pp. 211–219, May 2007, doi: 10.1016/j.tins.2007.03.001.
[47] K. A. Jellinger, “Is Braak staging valid for all types of Parkinson’s disease?,” *J. Neural Transm. Vienna Austria 1996*, vol. 126, no. 4, pp. 423–431, Apr. 2019, doi: 10.1007/s00702-018-1898-9.
[48] L. Parkkinen, T. Pirttilä, and I. Alafuzoff, “Applicability of current staging/categorization of α-synuclein pathology and their clinical relevance,” *Acta Neuropathol. (Berl.)*, vol. 115, no. 4, pp. 399–407, Apr. 2008, doi: 10.1007/s00401-008-0346-6.
[49] P. Borghammer and N. Van Den Berge, “Brain-First versus Gut-First Parkinson’s Disease: A Hypothesis,” *J. Park. Dis.*, vol. 9, no. s2, pp. S281–S295, Jan. 2019, doi: 10.3233/JPD-191721.
[50] P. Borghammer *et al.*, “Neuropathological evidence of body-first vs. brain-first Lewy body disease,” *Neurobiol. Dis.*, vol. 161, p. 105557, Dec. 2021, doi: 10.1016/j.nbd.2021.105557.
[51] J. Horsager *et al.*, “Brain-first versus body-first Parkinson’s disease: a multimodal imaging case-control study,” *Brain*, vol. 143, no. 10, pp. 3077–3088, Oct. 2020, doi: 10.1093/brain/awaa238.
[52] J. Horsager and P. Borghammer, “Brain-first vs. body-first Parkinson’s disease: An update on recent evidence,” *Parkinsonism Relat. Disord.*, vol. 122, p. 106101, May 2024, doi: 10.1016/j.parkreldis.2024.106101.
[53] E. E. Patton, L. I. Zon, and D. M. Langenau, “Zebrafish disease models in drug discovery: from preclinical modelling to clinical trials,” *Nat. Rev. Drug Discov.*, vol. 20, no. 8, pp. 611–628, Aug. 2021, doi: 10.1038/s41573-021-00210-8.
[54] S. Longkumer, A. Jamir, and P. Pankaj, “Maintenance and Breeding of Zebrafish under Laboratory Conditions for Animal Research,” *Agric. Sci. Dig. - Res. J.*, Aug. 2022, doi: 10.18805/ag.D-5599.
[55] T.-Y. Choi, T.-I. Choi, Y.-R. Lee, S.-K. Choe, and C.-H. Kim, “Zebrafish as an animal model for biomedical research,” *Exp. Mol. Med.*, vol. 53, no. 3, pp. 310–317, Mar. 2021, doi: 10.1038/s12276-021-00571-5.
[56] J. T. Shin and M. C. Fishman, “From Zebrafish to human: modular medical models,” *Annu. Rev. Genomics Hum. Genet.*, vol. 3, pp. 311–340, 2002, doi: 10.1146/annurev.genom.3.031402.131506.
[57] G. J. Lieschke and P. D. Currie, “Animal models of human disease: zebrafish swim into view,” *Nat. Rev. Genet.*, vol. 8, no. 5, pp. 353–367, May 2007, doi: 10.1038/nrg2091.
[58] A. L. Menke, J. M. Spitsbergen, A. P. M. Wolterbeek, and R. A. Woutersen, “Normal anatomy and histology of the adult zebrafish,” *Toxicol. Pathol.*, vol. 39, no. 5, pp. 759–775, Aug. 2011, doi: 10.1177/0192623311409597.
[59] G. Elizalde-Velázquez and S. Herrera-Vázquez, “Zebrafish as Model Organism in Aquatic Ecotoxicology: Current Trends and Future Perspectives,” 2023. doi: 10.5772/intechopen.1002731.
[60] M. M. Adams and H. Kafaligonul, “Zebrafish—A Model Organism for Studying the Neurobiological Mechanisms Underlying Cognitive Brain Aging and Use of Potential Interventions,” *Front. Cell Dev. Biol.*, vol. 6, Nov. 2018, doi:

10.3389/fcell.2018.00135.
[61] G. Zhai, J. Jia, C. Bereketoglu, Z. Yin, and A. Pradhan, “Sex-specific differences in zebrafish brains,” *Biol. Sex Differ.*, vol. 13, p. 31, Jun. 2022, doi: 10.1186/s13293-022-00442-2.
[62] C. D. Bonan and W. H. Norton, “The utility of zebrafish as a model for behavioural genetics,” *Curr. Opin. Behav. Sci.*, vol. 2, pp. 34–38, Apr. 2015, doi: 10.1016/j.cobeha.2014.07.003.
[63] M. B. Orger and G. G. de Polavieja, “Zebrafish Behavior: Opportunities and Challenges,” *Annu. Rev. Neurosci.*, vol. 40, no. Volume 40, 2017, pp. 125–147, Jul. 2017, doi: 10.1146/annurev-neuro-071714-033857.
[64] M. Adhish and I. Manjubala, “Effectiveness of zebrafish models in understanding human diseases—A review of models,” *Heliyon*, vol. 9, no. 3, p. e14557, Mar. 2023, doi: 10.1016/j.heliyon.2023.e14557.
[65] K. Howe *et al.*, “The zebrafish reference genome sequence and its relationship to the human genome,” *Nature*, vol. 496, no. 7446, pp. 498–503, Apr. 2013, doi: 10.1038/nature12111.
[66] Y. M. Bradford *et al.*, “Zebrafish Models of Human Disease: Gaining Insight into Human Disease at ZFIN,” *ILAR J.*, vol. 58, no. 1, pp. 4–16, Jul. 2017, doi: 10.1093/ilar/ilw040.
[67] C. L. Kemmler *et al.*, “Next-generation plasmids for transgenesis in zebrafish and beyond,” *Development*, vol. 150, no. 8, p. dev201531, Apr. 2023, doi: 10.1242/dev.201531.
[68] Y. Li, Z. Jia, S. Zhang, and X. He, “Progress in Gene-Editing Technology of Zebrafish,” *Biomolecules*, vol. 11, no. 9, p. 1300, Sep. 2021, doi: 10.3390/biom11091300.
[69] A. Urasaki, G. Morvan, and K. Kawakami, “Functional dissection of the Tol2 transposable element identified the minimal cis-sequence and a highly repetitive sequence in the subterminal region essential for transposition,” *Genetics*, vol. 174, no. 2, pp. 639–649, Oct. 2006, doi: 10.1534/genetics.106.060244.
[70] “Transient knockdown and overexpression reveal a developmental role for the zebrafish enosf1b gene | Cell & Bioscience | Full Text.” Accessed: Aug. 19, 2024. [Online]. Available: https://cellandbioscience.biomedcentral.com/articles/10.1186/2045-3701-1-32
[71] “Genome editing with engineered zinc finger nucleases | Nature Reviews Genetics.” Accessed: Aug. 19, 2024. [Online]. Available: https://www.nature.com/articles/nrg2842
[72] M. Christian *et al.*, “Targeting DNA double-strand breaks with TAL effector nucleases,” *Genetics*, vol. 186, no. 2, pp. 757–761, Oct. 2010, doi: 10.1534/genetics.110.120717.
[73] “CRISPR-Cas9-induced gene knockout in zebrafish - PMC.” Accessed: Aug. 19, 2024. [Online]. Available: https://www.ncbi.nlm.nih.gov/pmc/articles/PMC9617198/
[74] W. A. Sassen and R. W. Köster, “A molecular toolbox for genetic manipulation of zebrafish,” *Adv. Genomics Genet.*, vol. 5, pp. 151–163, Mar. 2015, doi: 10.2147/AGG.S57585.
[75] D. Balciunas *et al.*, “Harnessing a High Cargo-Capacity Transposon for Genetic Applications in Vertebrates,” *PLoS Genet.*, vol. 2, no. 11, p. e169, Nov. 2006, doi: 10.1371/journal.pgen.0020169.
[76] “Transposon tools hopping in vertebrates | Briefings in Functional Genomics | Oxford

Academic.” Accessed: Aug. 19, 2024. [Online]. Available: https://academic.oup.com/bfg/article/7/6/444/281770
[77] K. Kawakami, A. Shima, and N. Kawakami, “Identification of a functional transposase of the Tol2 element, an Ac-like element from the Japanese medaka fish, and its transposition in the zebrafish germ lineage,” *Proc. Natl. Acad. Sci. U. S. A.*, vol. 97, no. 21, pp. 11403–11408, Oct. 2000, doi: 10.1073/pnas.97.21.11403.
[78] S. Fisher *et al.*, “Evaluating the biological relevance of putative enhancers using Tol2 transposon-mediated transgenesis in zebrafish,” *Nat. Protoc.*, vol. 1, no. 3, pp. 1297–1305, 2006, doi: 10.1038/nprot.2006.230.
[79] K. M. Kwan *et al.*, “The Tol2kit: a multisite gateway-based construction kit for Tol2 transposon transgenesis constructs,” *Dev. Dyn. Off. Publ. Am. Assoc. Anat.*, vol. 236, no. 11, pp. 3088–3099, Nov. 2007, doi: 10.1002/dvdy.21343.
[80] K. J. Clark, M. D. Urban, K. J. Skuster, and S. C. Ekker, “Transgenic Zebrafish Using Transposable Elements,” *Methods Cell Biol.*, vol. 104, pp. 137–149, 2011, doi: 10.1016/B978-0-12-374814-0.00008-2.
[81] E. K. Don *et al.*, “A Tol2 Gateway-Compatible Toolbox for the Study of the Nervous System and Neurodegenerative Disease,” *Zebrafish*, vol. 14, no. 1, pp. 69–72, Feb. 2017, doi: 10.1089/zeb.2016.1321.
[82] O. Randlett *et al.*, “Whole-brain activity mapping onto a zebrafish brain atlas,” *Nat. Methods*, vol. 12, no. 11, pp. 1039–1046, Nov. 2015, doi: 10.1038/nmeth.3581.
[83] O. Wasel and J. L. Freeman, “Chemical and Genetic Zebrafish Models to Define Mechanisms of and Treatments for Dopaminergic Neurodegeneration,” *Int. J. Mol. Sci.*, vol. 21, no. 17, p. 5981, Aug. 2020, doi: 10.3390/ijms21175981.
[84] “Using the zebrafish model for Alzheimer’s disease research - PMC.” Accessed: Aug. 19, 2024. [Online]. Available: https://www.ncbi.nlm.nih.gov/pmc/articles/PMC4075077/
[85] J. M. Doyle and R. P. Croll, “A Critical Review of Zebrafish Models of Parkinson’s Disease,” *Front. Pharmacol.*, vol. 13, p. 835827, Mar. 2022, doi: 10.3389/fphar.2022.835827.
[86] N. A. S. Oliveira, B. R. Pinho, and J. M. A. Oliveira, “Swimming against ALS: How to model disease in zebrafish for pathophysiological and behavioral studies,” *Neurosci. Biobehav. Rev.*, vol. 148, p. 105138, May 2023, doi: 10.1016/j.neubiorev.2023.105138.
[87] X. Wang, J.-B. Zhang, K.-J. He, F. Wang, and C.-F. Liu, “Advances of Zebrafish in Neurodegenerative Disease: From Models to Drug Discovery,” *Front. Pharmacol.*, vol. 12, Jul. 2021, doi: 10.3389/fphar.2021.713963.
[88] D. Koehler and F. E. Williams, “Utilizing zebrafish and okadaic acid to study Alzheimer’s disease,” *Neural Regen. Res.*, vol. 13, no. 9, pp. 1538–1541, Sep. 2018, doi: 10.4103/1673-5374.237111.
[89] S. E. Nada, F. E. Williams, and Z. A. Shah, “Development of a Novel and Robust Pharmacological Model of Okadaic Acid-induced Alzheimer’s Disease in Zebrafish,” *CNS Neurol. Disord. Drug Targets*, vol. 15, no. 1, pp. 86–94, 2016, doi: 10.2174/1871527314666150821105602.
[90] R. K. Banote *et al.*, “Amyloid precursor protein-b facilitates cell adhesion during early development in zebrafish,” *Sci. Rep.*, vol. 10, no. 1, p. 10127, Jun. 2020, doi: 10.1038/s41598-020-66584-8.
[91] Y.-Z. Pu *et al.*, “Generation of Alzheimer’s Disease Transgenic Zebrafish Expressing Human APP Mutation Under Control of Zebrafish appb Promotor,” *Curr. Alzheimer*

Res., vol. 14, no. 6, pp. 668–679, 2017, doi: 10.2174/1567205013666161201202000.
[92] J. R. Morrice, C. Y. Gregory-Evans, and C. A. Shaw, "Animal models of amyotrophic lateral sclerosis: A comparison of model validity," *Neural Regen. Res.*, vol. 13, no. 12, pp. 2050–2054, Dec. 2018, doi: 10.4103/1673-5374.241445.
[93] M.-L. Campanari, A. Marian, S. Ciura, and E. Kabashi, "TDP-43 Regulation of AChE Expression Can Mediate ALS-Like Phenotype in Zebrafish," *Cells*, vol. 10, no. 2, p. 221, Jan. 2021, doi: 10.3390/cells10020221.
[94] E. T. McKinley, T. C. Baranowski, D. O. Blavo, C. Cato, T. N. Doan, and A. L. Rubinstein, "Neuroprotection of MPTP-induced toxicity in zebrafish dopaminergic neurons," *Brain Res. Mol. Brain Res.*, vol. 141, no. 2, pp. 128–137, Nov. 2005, doi: 10.1016/j.molbrainres.2005.08.014.
[95] V. Sallinen *et al.*, "MPTP and MPP+ target specific aminergic cell populations in larval zebrafish," *J. Neurochem.*, vol. 108, no. 3, pp. 719–731, Feb. 2009, doi: 10.1111/j.1471-4159.2008.05793.x.
[96] N. Sarath Babu, C. L. N. Murthy, S. Kakara, R. Sharma, C. V. Brahmendra Swamy, and M. M. Idris, "1-Methyl-4-phenyl-1,2,3,6-tetrahydropyridine induced Parkinson's disease in zebrafish," *Proteomics*, vol. 16, no. 9, pp. 1407–1420, May 2016, doi: 10.1002/pmic.201500291.
[97] A. A. Dukes *et al.*, "Live imaging of mitochondrial dynamics in CNS dopaminergic neurons in vivo demonstrates early reversal of mitochondrial transport following MPP(+) exposure," *Neurobiol. Dis.*, vol. 95, pp. 238–249, Nov. 2016, doi: 10.1016/j.nbd.2016.07.020.
[98] C. Parng, N. M. Roy, C. Ton, Y. Lin, and P. McGrath, "Neurotoxicity assessment using zebrafish," *J. Pharmacol. Toxicol. Methods*, vol. 55, no. 1, pp. 103–112, 2007, doi: 10.1016/j.vascn.2006.04.004.
[99] Y. Vijayanathan *et al.*, "6-OHDA-Lesioned Adult Zebrafish as a Useful Parkinson's Disease Model for Dopaminergic Neuroregeneration," *Neurotox. Res.*, vol. 32, no. 3, pp. 496–508, Oct. 2017, doi: 10.1007/s12640-017-9778-x.
[100] Y. Wang *et al.*, "Parkinson's disease-like motor and non-motor symptoms in rotenone-treated zebrafish," *NeuroToxicology*, vol. 58, pp. 103–109, Jan. 2017, doi: 10.1016/j.neuro.2016.11.006.
[101] T. E. Müller *et al.*, "Sodium Selenite Prevents Paraquat-Induced Neurotoxicity in Zebrafish," *Mol. Neurobiol.*, vol. 55, no. 3, pp. 1928–1941, Mar. 2018, doi: 10.1007/s12035-017-0441-6.
[102] D. Sheng *et al.*, "Deletion of the WD40 Domain of LRRK2 in Zebrafish Causes Parkinsonism-Like Loss of Neurons and Locomotive Defect," *PLoS Genet.*, vol. 6, no. 4, p. e1000914, Apr. 2010, doi: 10.1371/journal.pgen.1000914.
[103] M. E. Fett *et al.*, "Parkin is protective against proteotoxic stress in a transgenic zebrafish model," *PloS One*, vol. 5, no. 7, p. e11783, Jul. 2010, doi: 10.1371/journal.pone.0011783.
[104] S. Soman *et al.*, "Inhibition of the mitochondrial calcium uniporter rescues dopaminergic neurons in pink1-/- zebrafish," *Eur. J. Neurosci.*, vol. 45, no. 4, pp. 528–535, Feb. 2017, doi: 10.1111/ejn.13473.
[105] C. Milanese *et al.*, "Hypokinesia and reduced dopamine levels in zebrafish lacking β- and γ1-synucleins," *J. Biol. Chem.*, vol. 287, no. 5, pp. 2971–2983, Jan. 2012, doi: 10.1074/jbc.M111.308312.
[106] V. S. Van Laar *et al.*, "α-Synuclein amplifies cytoplasmic peroxide flux and oxidative stress provoked by mitochondrial inhibitors in CNS dopaminergic neurons

in vivo," *Redox Biol.*, vol. 37, p. 101695, Oct. 2020, doi: 10.1016/j.redox.2020.101695.
[107] A. Lopez, A. Gorb, N. Palha, A. Fleming, and D. C. Rubinsztein, "A New Zebrafish Model to Measure Neuronal α-Synuclein Clearance In Vivo," *Genes*, vol. 13, no. 5, p. 868, May 2022, doi: 10.3390/genes13050868.
[108] K. C. O'Donnell, A. Lulla, M. C. Stahl, N. D. Wheat, J. M. Bronstein, and A. Sagasti, "Axon degeneration and PGC-1α-mediated protection in a zebrafish model of α-synuclein toxicity," *Dis. Model. Mech.*, vol. 7, no. 5, pp. 571–582, May 2014, doi: 10.1242/dmm.013185.
[109] C. Mosimann, "Multisite Gateway Calculations: Excel spreadsheet," Feb. 2022, Accessed: Aug. 20, 2024. [Online]. Available: https://www.protocols.io/view/multisite-gateway-calculations-excel-spreadsheet-b4xdqxi6
[110] GBD 2016 Parkinson's Disease Collaborators, "Global, regional, and national burden of Parkinson's disease, 1990-2016: a systematic analysis for the Global Burden of Disease Study 2016," *Lancet Neurol.*, vol. 17, no. 11, pp. 939–953, Nov. 2018, doi: 10.1016/S1474-4422(18)30295-3.
[111] W. Oertel and J. B. Schulz, "Current and experimental treatments of Parkinson disease: A guide for neuroscientists," *J. Neurochem.*, vol. 139 Suppl 1, pp. 325–337, Oct. 2016, doi: 10.1111/jnc.13750.
[112] T. Pardo-Moreno *et al.*, "Current Treatments and New, Tentative Therapies for Parkinson's Disease," *Pharmaceutics*, vol. 15, no. 3, p. 770, Feb. 2023, doi: 10.3390/pharmaceutics15030770.
[113] J. Meiser, D. Weindl, and K. Hiller, "Complexity of dopamine metabolism," *Cell Commun. Signal. CCS*, vol. 11, p. 34, May 2013, doi: 10.1186/1478-811X-11-34.
[114] "Tissue expression of SNCA - Summary - The Human Protein Atlas." Accessed: Aug. 20, 2024. [Online]. Available: https://www.proteinatlas.org/ENSG00000145335-SNCA/tissue#rna_expression
[115] C. Mosimann, C. K. Kaufman, P. Li, E. K. Pugach, O. J. Tamplin, and L. I. Zon, "Ubiquitous transgene expression and Cre-based recombination driven by the ubiquitin promoter in zebrafish," *Dev. Camb. Engl.*, vol. 138, no. 1, pp. 169–177, Jan. 2011, doi: 10.1242/dev.059345.
[116] A. Landy, "Dynamic, structural, and regulatory aspects of lambda site-specific recombination," *Annu. Rev. Biochem.*, vol. 58, pp. 913–949, 1989, doi: 10.1146/annurev.bi.58.070189.004405.
[117] S. E. Riley, Y. Feng, and C. G. Hansen, "Hippo-Yap/Taz signalling in zebrafish regeneration," *Npj Regen. Med.*, vol. 7, no. 1, pp. 1–16, Jan. 2022, doi: 10.1038/s41536-022-00209-8.
[118] P. Borghammer, "The α-Synuclein Origin and Connectome Model (SOC Model) of Parkinson's Disease: Explaining Motor Asymmetry, Non-Motor Phenotypes, and Cognitive Decline," *J. Park. Dis.*, vol. 11, no. 2, pp. 455–474, Jan. 2021, doi: 10.3233/JPD-202481.

Appendix

Entry vector sequences

pME- α-syn

GAGGGAGCAGGGAGCATTGCAGCAGCCACTGGCTTTGTCAAAAAGGACCAGTTGGGCAAGAATGAAGAAGGAGCCCCAC
AGGAAGGAATTCTGGAAGATATGCCTGTGGATCCTGACAATGAGGCTTATGAAATGCCTTCTGAGGAAGGGTATCAAGA
CTACGAACCTGAAGCCTAAGAAATATCTTTGCTCCCAGTTTCTTGAGACCCAGCTTTCTTCTTGTACAAAGTTGGCATT
ATAAGAAAGCATTGCTTATCAATTTGTTGCAACGAACAGGTCACTATCAGTCAAAATAAAATCATTATTTGCCATCCAG
CTGATATCCCCTATAGTGAGTCGTATTACATGGTCATAGCTGTTTCCTGGCAGCTCTGGCCCGTGTCTCAAAATCTCTG
ATGTTACATTGCACAAGATAAAATAATATCATCATGAACAATAAAACTGTCTGCTTACATAAACAGTAATACAAGGGGT
GTTATGAGCCATATTCAACGGGAAACGTCGAGGCCGCGATTAAATTCCAACATGGATGCTGATTTATATGGGTATAAAT
GGGCTCGCGATAATGTCGGGCAATCAGGTGCGACAATCTATCGCTTGTATGGGAAGCCCGATGCGCCAGAGTTGTTTCT
GAAACATGGCAAAGGTAGCGTTGCCAATGATGTTACAGATGAGATGGTCAGACTAAACTGGCTGACGGAATTTATGCCT
CTTCCGACCATCAAGCATTTTATCCGTACTCCTGATGATGCATGGTTACTCACCACTGCGATCCCCGGAAAAACAGCAT
TCCAGGTATTAGAAGAATATCCTGATTCAGGTGAAAATATTGTTGATGCGCTGGCAGTGTTCCTGCGCCGGTTGCATTC
GATTCCTGTTTGTAATTGTCCTTTTAACAGCGATCGCGTATTTCGTCTCGCTCAGGCGCAATCACGAATGAATAACGGT
TTGGTTGATGCGAGTGATTTTGATGACGAGCGTAATGGCTGGCCTGTTGAACAAGTCTGGAAAGAAATGCATAAACTTT
TGCCATTCTCACCGGATTCAGTCGTCACTCATGGTGATTTCTCACTTGATAACCTTATTTTTGACGAGGGGAAATTAAT
AGGTTGTATTGATGTTGGACGAGTCGGAATCGCAGACCGATACCAGGATCTTGCCATCCTATGGAACTGCCTCGGTGAG
TTTTCTCCTTCATTACAGAAACGGCTTTTTCAAAAATATGGTATTGATAATCCTGATATGAATAAATTGCAGTTTCATT
TGATGCTCGATGAGTTTTTCTAATCAGAATTGGTTAATTGGTTGTAACACTGGCAGAGCATTACGCTGACTTGACGGGA
CGGCGCAAGCTCATGACCAAAATCCCTTAACGTGAGTTACGCGTCGTTCCACTGAGCGTCAGACCCCGTAGAAAAGATC
AAAGGATCTTCTTGAGATCCTTTTTTTCTGCGCGTAATCTGCTGCTTGCAAACAAAAAAACCACCGCTACCAGCGGTGG
TTTGTTTGCCGGATCAAGAGCTACCAACTCTTTTTCCGAAGGTAACTGGCTTCAGCAGAGCGCAGATACCAAATACTGT
TCTTCTAGTGTAGCCGTAGTTAGGCCACCACTTCAAGAACTCTGTAGCACCGCCTACATACCTCGCTCTGCTAATCCTG
TTACCAGTGGCTGCTGCCAGTGGCGATAAGTCGTGTCTTACCGGGTTGGACTCAAGACGATAGTTACCGGATAAGGCGC
AGCGGTCGGGCTGAACGGGGGGTTCGTGCACACAGCCCAGCTTGGAGCGAACGACCTACACCGAACTGAGATACCTACA
GCGTGAGCTATGAGAAAGCGCCACGCTTCCCGAAGGGAGAAAGGCGGACAGGTATCCGGTAAGCGGCAGGGTCGGAACA
GGAGAGCGCACGAGGGAGCTTCCAGGGGGAAACGCCTGGTATCTTTATAGTCCTGTCGGGTTTCGCCACCTCTGACTTG
AGCGTCGATTTTTGTGATGCTCGTCAGGGGGGCGGAGCCTATGGAAAAACGCCAGCAACGCGGCCTTTTTACGGTTCCT
GGCCTTTTGCTGGCCTTTTGCTCACATGTT

pENTR5-Ubi

```
TAACAAAGCAGTAGGCTTAAATAAACCTAATTTTTATAGGCTGTTCTCTACAACCCTCAAACAGTGATTAGTTTTGTACTTATAAACTTGCCCTTTCA
TTCATATTTCAAGAAAATTGGTTCAGAAGATCTGGATATTCTAGCAGTTGTTCAAGCTCATGGAGGGATCAGTGACCTGATTCCACAATGACTAGGCC
TAATCCAGAAATTAGATGACTGTCAACATAAAAAGGCACAGCACTCACTAGCTGCCCTATATATTTTATTATATTTTACATATATTATTTTATTTATT
TAGCTCTGAGTGCTGTACTTTCTGGTTAAAGAAAACTGCTTACAACAGCTAACCTGTACTACCTCAGGCTCAGGGAATTTGGAACAGGTTTGTCTGGT
TTGTTTCTTTAACCATGCATGCTTGTTTTCAACTATGGCAACACAGTCACATGGGACATTACAGAAATGATTTGTCGATGACATGCGACTTTTCTTTA
ATAAAGCGCAAAGATCCCAAAAAGCAAACTTTTAACAAAAATCATATAATTATATTTTCAATCCAGCTTTGTAGCAACTTTGTGCTGCTGTTCACTCA
GCAACAGATAGTCAGTATAAGGTCAGTGTGTCTCAAAGCAGTGCCATCTGTTTCACACATTGCGTTCTATATATAAGTGTGCTGGTTGACACGACACT
GTATAAGGCCTAGGCTAAAACACAAACAATGTAGAATGACACTGTGTTTTTTTTGTAAACAAATGTTGTTTTTGGTTAAACATCTTTGTGAAAACATC
CTCCTGTCATGTATTTGCTATATTCAAATGTTAAACCCGTGCAGAATAGAACATATACAAAAAAAAACAACACAACACATTTTTAAACATTATTAAAT
ATCAAGTATTGCTGGCAGTTCTGTTTCTGTTTTACAGTACCCTTTGCCACAGTTCTCCGCTTTTCCTGGTCCAGATTCCACAAGTCTGATTCACCAAT
AGCAAAGCGAATAAACAACCAAAGCAGCCAATCACTGCTTGTAGACTGTCCTGCGAGACCGGCCCATTCCAGCACATTCTGGAAACTTCCTTTATATG
ATAATTATAAATACATTTAAATTATTGATACAAAACATGTAATTCCTAGAACATAACCATAGCAATCATTAGTTTTCAGGGTAATTATGTATTTTTAG
GATTTGACTGCGGAAAGATCTGGTCATGTGACGTCTCATGAACGTCACGGCCCTGGGTTTCTATAAATACAGTAGGACTCTCGACCATCGGCAGATTT
TTCGAAGAAGAAGATCAGTTTCAGGAGCCGTACTGTTCCGTTTCAACGCAAATATTAACGGTAAGAGCGAATTTCCTAGTTTGTTTTCATGCCATTCT
TTAAAACCATAGCGTATTACTTTAATTATAGTAAACTTTCGCTTTCTTTATTACAAGAGACGTTTTGTGTTGATTCTCCGCGGACATTTTCGGTCAGA
CAATCAGAAAATGACCGCGGAGGACCAGTAACTTGCATTACACGTAAGTTAAATCTTCGTGTATTAAAATGGTTAGGTTGTTAACGTCAAATAGGTTA
CCGTGTTTGCGTGTGATCAGGTTGGTTTTGTTAGATTTTTGTCAGTATTTTTAATTTATTTGTTTTAGTTTATTTATTTTTTTTGCTGAATCATAGTT
TGTGAACAAAGAACCCGGATGTTACATACAGTACAGCCGCCATGTTACAGAGAGTTATAACTTAATCATTTTAAAAATAATTTTGCCTTACTTTTAGT
TTGTCATGTTGAGAAATGAGGAAATGTTAAAATGAGGAAATATCCAATTAATTTAATATATCAAAATAATCCATGATTACAATGCACTGAACTGGAGA
AAATTAAGATGTTTTCTAGTGTCATGAAACAAATGTAAGAGATGTACATTGTAGATGTTTTATGTCAAGAATTGGCTAGTTGATGCAGCATACTGGCG
ATACTCAGTTGTAATAACAGTAACGTTACATGTTAATAGACTACTGAGTATGCTGTTCTGTCTATGTATGCTCTGTAAGCTACGAGAAGGACTTTTTT
AAACAGTAAAGGGTGCAATATTTTTACAAATTGAATTAAATAAAGGCTGTCTATTAAGTAATATGCTTGATATTTTTCTTACTTGATCGGAAATAAGA
AAAAATATAAACGTTGTTGCTCTAAAAATCCTAGTTCAGTTTAGCCAACCACAAATACCTTTTTGTTCCTCCAACAGTTTTTTTTTCTTCTCTATAAT
ATTTGGCAGTCTATAGTACTCCAAATGTTTCCCCACAGTCTAACTAATTGGTACAGCCAAAATCATGACACTTATTGCAATAATAATTTTGGTTCATT
GGCATTGTTGATAGCCTGTGCCACTAATATGGTCGATTGATCATGCTTCAGGAAGAAAACTATATTGTTTGATGTAAGATTATTAAATCTTCACCTGC
TTCCATTACAAACTATTCCCATCTTATTGAATTCTGGTATGTCTTAAAGGATTAGTTCACTTCCCAAATCAAAATTTACTTAGCCTTTTTTCATCCAT
GATCCCTTTTTTTCATCATTAATGAAGAAATTGTTTTTGAAAAAGTTTCAAGATTTTTTTCTCTATATTGTGGAGCTTGTTAGTTTAAAATTCCAAAA
TGCAATATGTGGCTTCAAATGGTTCTAAATGATCCCAGTCAAGGAATAACAGTCTTATCTAATGAAACCATTAGACCTTTAAAAATAAAAAAAATAAA
AGTATTTATTTTTAAATGACTGAGTGATTAAGTTGAATTTCAGCGTTTCCTTACTGTGTAGAAGTCCTTCCTTACTGGCCCCACCCTTTGGTTCTCTG
CCAATCTGCTACCTAATGTAATGTTGTGGAACATTATTATTCTTTATTTCTTAATTTTTTATTTTTTATTTTAAAACAATGTAAACTGCACAGATGTG
CAGTTTGTTTAAAATGGCCAATGCTTTGGAAATGCATGACATAATTAGATTTCATGATGCACAAAGCCAAATCTCAGAGCTTGTGCAAAATGAGCTAT
CATTTCACTAGGTAAGACCCTAAATTTTCATATAGGATCATTTGGACAATTTTGCTGCAGGTAAAATGCATTCTATAGTCCACTGTCAGCCATTGTTT
TGGATAGTATTTATTTTTCTCTACAAGTATAGTCAATAGTTTTCTATTATTTTAAAGGTTTGTAACATTTAAGGGTGACCAAATGCAAAGTAAAATTT
CATTTTCGGGTGAACTATCTCGTTTAACATGGGAGAAGTGCAAAACATACATTATTGGCTAGAACATTGTAGTATTTTTTAAATGGAAATGTGTGATT
GCTAATCTTACTTTGAATTTGTTTACAGGGATCCTTTAAGGGCGAATTCGACCCAAGTTTGTAC
```

P3E-mCherry

```
TTTACAGTATTATGTAGTCTGTTTTTTATGCAAAATCTAATTTAATATATTGATATTTATATCATTTTACGTTTCTCGTTCAACTTTCTTGTACAAAGT
GGTTATGGTGAGCAAGGGCGAGGACGACAACATGGCCATCATCAAGGAGTTCATGCGCTTCAAGGTGCACATGGAGGGCTCCGTGAACGGCCACGAGTT
CGAGATCGAGGGCGAGGGCGAGGGCCGCCCCTACGAGGGCACCCAGACCGCCAAGCTGAAGGTGACCAAGGGCGGCCCCCTGCCCTTCGCCTGGGACAT
CCTGTCCCCTCAGTTCATGTACGGCTCCAAGGCCTACGTGAAGCACCCCGCCGACATCCCCGACTACTTGAAGCTGTCCTTCCCCGAGGGCTTCAAGTG
GGAGCGCGTGATGAACTTCGAGGACGGCGGCGTGGTGACCGTGACCCAGGACTCCTCCCTGCAGGACGGCGAGTTCATCTACAAGGTGAAGCTGCGCGG
CACCAACTTCCCCTCCGACGGCCCCGTAATGCAGAAGAAGACCATGGGCTGGGAGGCCTCCTCCGAGCGGATGTACCCCGAGGACGGCGCCCTGAAGGG
CGAGATCAAGCAGAGGCTGAAGCTGAAGGACGGCGGCCACTACGACGCCGAGGTCAAGACCACCTACAAGGCCAAGAAGCCCGTGCAGCTGCCCGGCGC
CTACAACGTCAACATCAAGCTGGACATCACCTCCCACAACGAGGACTACACCATCGTGGAACAGTACGAGCGCGCCGAGGGCCGCCACTCCACCGGCGG
CATGGACGAGCTGTACAAGTAAGGCGCGCCTCTAGAACTATAGTGAGTCGTATTACGTAGATCCAGACATGATAAGATACATTGATGAGTTTGGACAAA
CCACAACTAGAATGCAGTGAAAAAAATGCTTTATTTGTGAAATTTGTGATGCTATTGCTTTATTTGTAACCATTATAAGCTGCAATAAACAAGTTAACA
ACAACAATTGCATTCATTTTATGTTTCAGGTTCAGGGGGAGGTGTGGGAGGTTTTTTCCAACTTTATTATACAAAGTTGGCATTATAAAAAAGCATTGC
TTATCAATTTGTTGCAACGAACAGGTCACTATCAGTCAAAATAAAATCATTATTTGGAGCTCCATGGTAGCGTTAACGCGGCCGCGATATCCCCTATAG
TGAGTCGTATTACATGGTCATAGCTGTTTCCTGGCAGCTCTGGCCCGTGTCTCAAAATCTCTGATGTTACATTGCACAAGATAAAAATATATCATCATG
AACAATAAAACTGTCTGCTTACATAAACAGTAATACAAGGGGTGTTATGAGCC
```